
Transferable Calibration with Lower Bias and Variance in Domain Adaptation

Ximei Wang, Mingsheng Long*, Jianmin Wang, and Michael I. Jordan[#]

School of Software, KLiss, BNRist, Tsinghua University [#]University of California, Berkeley
wxm17@mails.tsinghua.edu.cn {mingsheng, jimwang}@tsinghua.edu.cn
jordan@cs.berkeley.edu

Abstract

Domain Adaptation (DA) enables transferring a learning machine from a labeled source domain to an unlabeled target one. While remarkable advances have been made, most of the existing DA methods focus on improving the target accuracy at inference. How to estimate the predictive uncertainty of DA models is vital for decision-making in safety-critical scenarios but remains the boundary to explore. In this paper, we delve into the open problem of *Calibration in DA*, which is extremely challenging due to the coexistence of domain shift and the lack of target labels. We first reveal the dilemma that DA models learn higher accuracy at the expense of well-calibrated probabilities. Driven by this finding, we propose Transferable Calibration (TransCal) to achieve more accurate calibration with lower bias and variance in a unified hyperparameter-free optimization framework. As a general post-hoc calibration method, TransCal can be easily applied to recalibrate existing DA methods. Its efficacy has been justified both theoretically and empirically.

1 Introduction

Deep neural networks (DNNs) achieve the state of the art predictive accuracy in machine learning tasks with the benefit of powerful ability to learn discriminative representations [36, 12, 60]. However, in real-world scenarios, it is hard (intolerably time-consuming and labor-expensive) to collect sufficient labeled data through manual labeling, causing DNNs to confront challenges when generalizing the pre-trained model to a different domain with unlabeled data. To tackle this challenge, researchers propose to transfer knowledge from a different but related domain by leveraging the readily-available labeled data, a.k.a. domain adaptation (DA) [45].

There are mainly two types of domain adaptation formulas: *covariate shift* [45, 38, 30, 14] and *label shift* [28, 2, 1], while we focus on the former in this paper since it appears more natural in recognition tasks and attracts more attention in the literature. Early domain adaptation methods bridge the source and target domains mainly by learning domain-invariant representations [38, 17] or instance importances [24, 16]. After the breakthrough in deep neural networks (DNNs) has been achieved, they are widely believed to be able to learn more transferable features [36, 12, 60, 65], since they disentangle explanatory factors of variations. Recent works in deep domain adaptation can be mainly grouped into two categories: 1) *moment matching*. These methods align representations across domains by minimizing the discrepancy between feature distributions [53, 30, 32, 33, 29]; 2) *adversarial training*. These methods adversarially learn transferable feature representations by confusing a domain discriminator in a two-player game [15, 52, 31, 57, 64].

While numerous domain adaptation methods have been proposed, most of them mainly focus on improving the accuracy in the target domain but fail to estimate the predictive uncertainty, falling

*Corresponding author: Mingsheng Long (mingsheng@tsinghua.edu.cn)

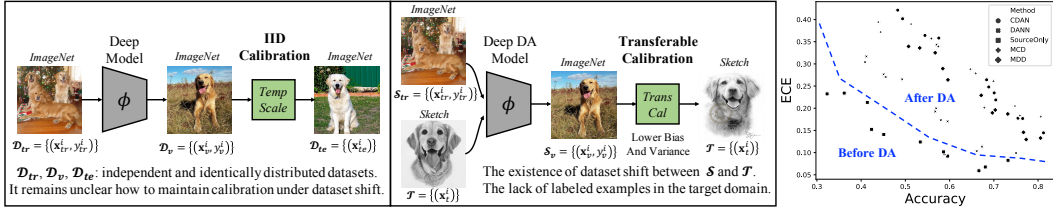


Figure 1: **Left:** A comparison between IID Calibration with TransCal, where ϕ denotes the deep model; **Right:** an observation on the accuracy and ECE of various DA methods (12 transfer tasks of Office-Home [54] with ResNet-50 [23]), indicating that DA models learn higher accuracy than the SourceOnly ones *at the expense of* well-calibrated probabilities. See more results in D.1 of Appendix.

short of a miscalibration problem [21]. The accuracy of a deep adapted model constitutes only one side of the coin, here we delve into the other side of the coin, i.e. *the calibration of accuracy and confidence*, which requires the model to output a probability that reflects the true frequency of an event. For example, if an automated diagnosis system says 1,000 patients have lung cancer with probability 0.1, approximately 100 of them should indeed have lung cancer. Calibration is fundamental to deep neural models and of great significance for decision-making in safety-critical scenarios. With built-in [13, 26] or post-hoc [43, 21] recalibration methods, the confidence and accuracy of deep models can be well-calibrated in the independent and identically distributed (IID) scenarios. However, it remains unclear how to maintain calibration under dataset shifts, especially when we do not have labels from the target dataset, as in the general setting of Unsupervised Domain Adaptation (UDA). We identify two obstacles in the way of applying calibration to UDA:

- *The lack of labeled examples in the target domain.* We know that the existing successful post-hoc IID recalibration methods mostly rely on ground-truth labels in the validation set to select the optimal temperature [43, 21]. However, since ground-truth labels are not available in the target domain, it is not feasible to directly apply IID calibration methods to UDA.
- *Dataset shift entangled with the miscalibration of DNNs.* Since DNNs are believed to learn more transferable features [36, 60], many domain adaptation methods embed DNNs to implicitly close the domain shift and rely on DNNs to achieve higher classification accuracy. However, DNNs are prone to over-confidence [21], falling short of a miscalibration problem.

To this end, we study the open problem of *Calibration in DA*, which is extremely challenging due to the coexistence of the domain gap and the lack of target labels. To figure out the calibration error on the target domain of DA models, we first delve into the predictions and confidences of the target dataset. By calculating the target accuracy and ECE [21] (a calibration error measure defined in 3.1) with various domain adaptation models before calibration, we found something interesting. As shown in the right panel of Figure 1, the accuracy increases from the weakest SourceOnly [23] model to the latest state-of-the-art MDD [64] model, while the ECE becomes larger as well. That is, after applying domain adaptation methods, miscalibration phenomena become severer compared with SourceOnly model, indicating that the domain adaptation models learn higher classification accuracy *at the expense of* well-calibrated probabilities. This dilemma is unacceptable in safety-critical scenarios, as we need higher accuracy while maintaining calibration. Worse still, the well-performed calibration methods in the IID setting cannot be directly applied to DA due to the domain shift.

To tackle the dilemma between accuracy and calibration, we propose a new Transferable Calibration (TransCal) method in DA, achieving more accurate calibration with lower bias and variance in a unified hyperparameter-free optimization framework, while a comparison with IID calibration is shown in the left panel of Figure 1. Specifically, we first define a new calibration measure, *Importance Weighted Expected Calibration Error* (IWECE) to estimate the calibration error in the target domain in a transferable calibration framework. Next, we propose a *learnable meta parameter* to further reduce the estimation bias from the perspective of theoretical analysis. Meanwhile, we develop a *serial control variate* method to further reduce the variance of the estimated calibration error. As a general post-hoc calibration method, TransCal can be easily applied to recalibrate existing DA methods. This paper has the following contributions:

- We uncover a dilemma in the open problem of Calibration in DA: existing domain adaptation models learn higher classification accuracy *at the expense of* well-calibrated probabilities.

- We propose a Transferable Calibration (TransCal) method, achieving more accurate calibration with lower bias and variance in a unified hyperparameter-free optimization framework.
- We conduct extensive experiments on various DA methods, datasets, and calibration metrics, while the effectiveness of our method has been justified both theoretically and empirically.

2 Related Work

2.1 Domain Adaptation

There are mainly two types of domain adaptation formulas: *covariate shift* [45, 38, 30, 14] and *label shift* [28, 2, 1], while we focus on the former in this paper since it appears more natural in recognition tasks and attracts more attention in the literature. Existing domain adaptation methods can be mainly grouped into two categories: *moment matching* and *adversarial training*. Moment matching methods align feature distributions across domains by minimizing the distribution discrepancy, in which Maximum Mean Discrepancy [20] is adopted by DAN [30] and DDC [53], and Joint Maximum Mean Discrepancy is utilized by JAN [33]. Motivated by Generative Adversarial Networks (GAN) [18], DANN [15] introduces a domain discriminator to distinguish the source features from the target ones, which are generated by the feature extractor. The domain discriminator and feature extractor are competing in a two-player minimax game. Further, CDAN [31] conditions the adversarial domain adaptation models on discriminative information conveyed in the classifier predictions. MADA [40] uses multiple domain discriminators to capture multimodal structures for fine-grained domain alignment. ADDA [52] adopts asymmetric feature extractors while MCD [49] employs two classifiers consistent across domains. MDD [64] proposes a new domain adaptation margin theory and achieves an impressive performance. TransNorm [56] tackles domain adaptation from a new perspective of designing a transferable normalization layer. Though numerous DA methods have been proposed, most of them focus on improving target accuracy and rare attention has been paid to the predictive uncertainty, causing a miscalibration between accuracy and confidence.

Table 1: Comparisons among calibration methods for unsupervised domain adaptation (UDA).

Calibration Method	works with domain shift	works without target label	Bias Reduction	Variance Reduction
Temp. Scaling [21]	✗	✗	✗	✗
MC-dropout [13]	✓	✗	✗	✗
CPCS [39]	✓	✓	✗	✗
TransCal (proposed)	✓	✓	✓	✓

2.2 Calibration

Among *binary* calibration methods, Histogram Binning [62] is a simple non-parametric one with either equal-width or equal-frequency bins; Isotonic Regression [63] is a strict generalization of histogram binning by jointly optimizing the bin boundaries and bin predictions; Differently, Platt Scaling [43] is a parametric one that transforms the logits of a classifier to probabilities. When extended to *multiclass*, there are two types of methods. 1) *built-in methods*: Monte Carlo dropout (MC-dropout) [13] is popular as it simply uses Dropout [50] during testing phase to estimate predictive uncertainty. Later, [26] finds out that the ensembles of neural networks can work. Further, Stochastic Variational Bayesian Inference (SVI) methods for deep learning [5, 34, 58] are shown effective. However, built-in methods require to modify the classifier learning algorithm or training procedure, which are complex to apply in DA. Thus, we prefer 2) *post-hoc approaches*, including various multi-class extensions of Platt scaling [43]: matrix scaling, vector scaling and temperature scaling [21]. Though remarkable advances of IID calibration are witnessed, it remains unclear how to maintain calibration under dataset shifts [25], especially when the target labels are unavailable in UDA case. Recently, [37] finds that traditional post-hoc IID recalibration methods such as temperature scaling fail to maintain calibration under distributional shift. A recent paper (CPCS) [39] considering calibration under dataset shift uses importance weighting to correct for the shift from the source to the target distribution and applies domain adaptation as a base tool for alignment, while we focus on how to maintain calibration in DA. A detailed comparison of typical calibration methods is shown in Table 1.

3 Approach

Let \mathbf{x} denote the input of the network, \mathbf{y} be the label and d be the Bernoulli variable indicating to which domain \mathbf{x} belongs. In our terminology, the source domain distribution is $p(\mathbf{x})$ and the target domain distribution is $q(\mathbf{x})$. We are given a labeled source domain $\mathcal{S} = \{(\mathbf{x}_s^i, \mathbf{y}_s^i)\}_{i=1}^{n_s}$ with n_s samples ($d = 1$), and an unlabeled target domain $\mathcal{T} = \{(\mathbf{x}_t^i)\}_{i=1}^{n_t}$ with n_t samples ($d = 0$). Similar to IID calibration, \mathcal{S} is first partitioned into $\mathcal{S}_{tr} = \{(\mathbf{x}_{tr}^i, \mathbf{y}_{tr}^i)\}_{i=1}^{n_{tr}}$ and $\mathcal{S}_v = \{(\mathbf{x}_v^i, \mathbf{y}_v^i)\}_{i=1}^{n_v}$. In this paper, we proposed a new Transferable Calibration (TransCal) method in DA under the well-known covariate shift assumption, *i.e.*, the equation $p(\mathbf{y}|\mathbf{x}) = q(\mathbf{y}|\mathbf{x})$ is held.

3.1 IID Calibration

Calibration Metrics. Given a deep neural model ϕ (parameterized by θ) which transforms the random variable input X into the class prediction \hat{Y} and its associated confidence \hat{P} , we can define the *perfect calibration* [21] as $\mathbb{P}(\hat{Y} = Y | \hat{P} = c) = c, \forall c \in [0, 1]$ where Y is the ground truth label. There are some typical metrics to measure calibration error: **1)** Negative Log-Likelihood (NLL) [19], also known as the cross-entropy loss in field of deep learning, serves as a proper scoring rule to measure the quality of a probabilistic model [22]. **2)** Brier Score (BS) [6], defined as the squared error between $p(\hat{\mathbf{y}}|\mathbf{x}, \theta)$ and \mathbf{y} , is another proper scoring rule for uncertainty measurement. **3)** Expected Calibration Error (ECE) [35, 21] first partitions the interval of probability predictions into B bins where B_m is the indices of samples falling into the m -th bin, and then computes the weighted absolute difference between accuracy and confidence across bins:

$$\mathcal{L}_{\text{ECE}} = \sum_{m=1}^B \frac{|B_m|}{n} |\mathbb{A}(B_m) - \mathbb{C}(B_m)|, \quad (1)$$

where for each bin m , the accuracy is $\mathbb{A}(B_m) = |B_m|^{-1} \sum_{i \in B_m} \mathbf{1}(\hat{\mathbf{y}}_i = \mathbf{y}_i)$ and its confidence is $\mathbb{C}(B_m) = |B_m|^{-1} \sum_{i \in B_m} \max_k p(\hat{\mathbf{y}}_i^k | \mathbf{x}_i, \theta)$. ECE is easier to interpret and thereby more popular.

Temperature Scaling Calibration. Temperature scaling is one of the simplest, fastest, and effective IID Calibration methods [21]. Fixing the neural model trained on the training set \mathcal{D}_{tr} , temperate scaling first attains the optimal temperature T^* by minimizing the cross-entropy loss between the logit vectors \mathbf{z}_v scaled by temperature T and the ground truth label \mathbf{y}_v on the validation set \mathcal{D}_v as

$$T^* = \arg \min_T \mathbb{E}_{(\mathbf{x}_v, \mathbf{y}_v) \in \mathcal{D}_v} \mathcal{L}_{\text{NLL}}(\sigma(\mathbf{z}_v/T), \mathbf{y}_v), \quad (2)$$

where $\sigma(\cdot)$ is the *softmax* function as $\sigma(z_j) = \exp(z_j) / \sum_{k=1}^K \exp(z_k)$ for K classes. After that, we transform the logit vectors \mathbf{z}_{te} on the test set \mathcal{D}_{te} into calibrated probabilities by $\hat{\mathbf{y}}_{te} = \sigma(\mathbf{z}_{te}/T^*)$.

3.2 Transferable Calibration Framework

As mentioned above, the main challenge of extending temperature scaling method into domain adaptation (DA) setup is that the target calibration error $\mathbb{E}_q = \mathbb{E}_{\mathbf{x} \sim q} [\mathcal{L}_{(\cdot)}(\phi(\mathbf{x}), \mathbf{y})]$ is defined over the target distribution q where labels are inaccessible. However, if density ratio (a.k.a. importance weight) $w(\mathbf{x}) = q(\mathbf{x})/p(\mathbf{x})$ is known, we can estimate target calibration error by the source distribution p :

$$\begin{aligned} \mathbb{E}_{\mathbf{x} \sim q} [\mathcal{L}_{(\cdot)}(\phi(\mathbf{x}), \mathbf{y})] &= \int_q \mathcal{L}_{(\cdot)}(\phi(\mathbf{x}), \mathbf{y}) q(\mathbf{x}) d\mathbf{x} \\ &= \int_p \frac{q(\mathbf{x})}{p(\mathbf{x})} \mathcal{L}_{(\cdot)}(\phi(\mathbf{x}), \mathbf{y}) p(\mathbf{x}) d\mathbf{x} = \mathbb{E}_{\mathbf{x} \sim p} [w(\mathbf{x}) \mathcal{L}_{(\cdot)}(\phi(\mathbf{x}), \mathbf{y})], \end{aligned} \quad (3)$$

which means $\mathbb{E}_{\mathbf{x} \sim p} [w(\mathbf{x}) \mathcal{L}_{(\cdot)}(\phi(\mathbf{x}), \mathbf{y})]$ is an *unbiased* estimator of the target calibration error \mathbb{E}_q . In Eq. (3), it is obvious that there are two building blocks: importance weight $w(\mathbf{x})$ and calibration metric $\mathcal{L}_{(\cdot)}$. We first delve into the specific type of calibration metric $\mathcal{L}_{(\cdot)}$. The existing calibration method under covariate shift (CPCS) [39] utilizes the Brier Score \mathcal{L}_{BS} . However, Brier Score conflates accuracy with calibration since it can be decomposed into two components: calibration error and refinement [11], making it insensitive to predicted probabilities associated with infrequent

events [37]. Meanwhile, NLL is minimized if and only if the prediction recovers ground truth \mathbf{y} , however, it may over-emphasize tail probabilities [7]. Hence, we adopt ECE, an intuitive and informative calibration metric to directly quantify the goodness of calibration. One may concern that ECE is not a proper scoring rule since the optimum score may not correspond to a perfect prediction, however, as a post-hoc method that softens the overconfident probabilities but *keeps the probability order over classes*, the temperature scaling we utilize will maintain the same accuracy with that before calibration, while achieving a lower ECE as shown in Fig. 2. Since this kind of calibration is trained on the source data but can transfer to the target domain, we call it *transferable calibration*.

Previously, we assume that density ratio is known, however, it is not readily accessible in real-world applications. In this paper, we adopt a mainstream discriminative density ratio estimation method: LogReg [44, 3, 8], which uses Bayesian formula to derive the estimated density ratio from a logistic regression classifier that separates examples from the source and the target domains as

$$\hat{w}(\mathbf{x}) = \frac{q(\mathbf{x})}{p(\mathbf{x})} = \frac{v(\mathbf{x}|d=0)}{v(\mathbf{x}|d=1)} = \frac{P(d=1)P(d=0|\mathbf{x})}{P(d=0)P(d=1|\mathbf{x})}, \quad (4)$$

where v is a distribution over $(\mathbf{x}, d) \in \mathcal{X} \times \{0, 1\}$ and $d \sim \text{Bernoulli}(0.5)$ is a Bernoulli variable indicating to which domain \mathbf{x} belongs. With Eq. (4), the estimated density ratio $\hat{w}(\mathbf{x})$ can be decomposed into two parts, in which the first part $P(d=1)/P(d=0)$ is a constant weight factor that can be estimated with the sample sizes of source and target domains as n_s/n_t , and the second part $P(d=0|\mathbf{x})/P(d=1|\mathbf{x})$ is the ratio of target probability to source probability that can be directly estimated with the probabilistic predictions of the logistic regression classifier. For simplicity, we randomly upsample the source or the target dataset to make $n_s = n_t$, i.e., $P(d=1)/P(d=0)$ equals to 1.0. In this way, $\hat{w}(\mathbf{x})$ is only decided by the second part: $P(d=0|\mathbf{x})/P(d=1|\mathbf{x})$.

3.3 Bias Reduction by Learnable Meta Parameter

Through the above analysis, we can reach an *unbiased* estimation of the target calibration error if the estimated importance weights are equal to the true ones. However, the gap between them are non-ignorable, causing a *bias* between the estimated calibration error and the ground-truth calibration error in the target domain. We formalize this bias of calibration as

$$\begin{aligned} \left| \mathbb{E}_{\mathbf{x} \sim q} \left[\mathcal{L}_{\text{ECE}}^{\hat{w}(\mathbf{x})} \right] - \mathbb{E}_{\mathbf{x} \sim q} \left[\mathcal{L}_{\text{ECE}}^{w(\mathbf{x})} \right] \right| &= \left| \mathbb{E}_{\mathbf{x} \sim p} [\hat{w}(\mathbf{x}) \mathcal{L}_{\text{ECE}}(\phi(\mathbf{x}), \mathbf{y})] - \mathbb{E}_{\mathbf{x} \sim p} [w(\mathbf{x}) \mathcal{L}_{\text{ECE}}(\phi(\mathbf{x}), \mathbf{y})] \right| \\ &= \left| \mathbb{E}_{\mathbf{x} \sim p} [(w(\mathbf{x}) - \hat{w}(\mathbf{x})) \mathcal{L}_{\text{ECE}}(\phi(\mathbf{x}), \mathbf{y})] \right|. \end{aligned} \quad (5)$$

Note that the bias of estimated calibration error in the target domain is highly related to the estimation error of importance weights. Hence, we focus on the bias of importance weights and show that after applying some basic mathematical inequalities, the estimation bias can be bounded by

$$\begin{aligned} & \left| \mathbb{E}_{\mathbf{x} \sim p} [(w(\mathbf{x}) - \hat{w}(\mathbf{x})) \mathcal{L}_{\text{ECE}}(\phi(\mathbf{x}), \mathbf{y})] \right| \\ & \leq \sqrt{\mathbb{E}_{\mathbf{x} \sim p} [(w(\mathbf{x}) - \hat{w}(\mathbf{x}))^2] \mathbb{E}_{\mathbf{x} \sim p} [(\mathcal{L}_{\text{ECE}}(\phi(\mathbf{x}), \mathbf{y}))^2]} \quad (\text{Cachy - Schwarz Inequality}) \\ & \leq \frac{1}{2} (\mathbb{E}_{\mathbf{x} \sim p} [(w(\mathbf{x}) - \hat{w}(\mathbf{x}))^2] + \mathbb{E}_{\mathbf{x} \sim p} [(\mathcal{L}_{\text{ECE}}(\phi(\mathbf{x}), \mathbf{y}))^2]) \quad (\text{AM/GM Inequality}) \end{aligned} \quad (6)$$

where AM/GM denotes the inequality of arithmetic and geometric means. It is noteworthy that the domain adaptation model ϕ is fixed since we consider transferable calibration as a post-hoc method. Therefore, we can safely bypass the second term of Eq. (6) and focus our attention on the first term. According to the standard *bounded importance weight assumption* [9], for some bound $M > 0$ we have $w(\mathbf{x}) \leq M$. Then for any \mathbf{x} s.t. $P(d=1|\mathbf{x}) \neq 0$, the following inequality holds:

$$\frac{1}{M+1} \leq P(d=1|\mathbf{x}) \leq 1, \quad \text{since } w(\mathbf{x}) = \frac{P(d=0|\mathbf{x})}{P(d=1|\mathbf{x})} = \frac{1 - P(d=1|\mathbf{x})}{P(d=1|\mathbf{x})} = \frac{1}{P(d=1|\mathbf{x})} - 1. \quad (7)$$

In this way, the first term of the bias in importance weights in Eq. (6) can be further bounded by

$$\begin{aligned} \mathbb{E}_{\mathbf{x} \sim p} [(w(\mathbf{x}) - \hat{w}(\mathbf{x}))^2] &= \mathbb{E}_{\mathbf{x} \sim p} \left[\left(\frac{P(d=1|\mathbf{x}) - \hat{P}(d=1|\mathbf{x})}{P(d=1|\mathbf{x})\hat{P}(d=1|\mathbf{x})} \right)^2 \right] \\ &\leq (M+1)^4 \mathbb{E}_{\mathbf{x} \sim p} \left[\left(P(d=1|\mathbf{x}) - \hat{P}(d=1|\mathbf{x}) \right)^2 \right]. \end{aligned} \quad (8)$$

Plugging Eq. (8) into Eq. (6), we conclude that a smaller M can ensure a lower bias for the estimated weight $\hat{w}(\mathbf{x})$, leading to a smaller bias of the estimated target calibration error, which is also supported by the generalization bound for importance weighting domain adaptation (Theorem 1, [9]).

To this end, what we should do is to find some techniques to control the upper bound M of importance weights. It seems that we can normalize each weight by the sum of all weights, leading to a smaller M . Still, only with self-normalization, a few bad samples with very large weights will dominate the estimation, and drastically explode the estimator. Further, can we clip those samples with very large weights by a given threshold? It seems feasible, but the threshold is task-specific and hard to preset, which is not an elegant solution that we pursue. Based on the above theoretical analysis, we propose to introduce a learnable meta parameter λ ($0 \leq \lambda \leq 1$) to adaptively downscale the extremely large weights, which can decrease M and attain a bias-reduced target calibration error. Formally,

$$T^* = \arg \min_{T, \lambda} \mathbb{E}_{\mathbf{x}_v \sim p} [\tilde{w}(\mathbf{x}_v) \mathcal{L}_{\text{ECE}}(\sigma(\phi(\mathbf{x}_v)/T), \mathbf{y})], \quad \tilde{w}(\mathbf{x}_v^i) = [\hat{w}(\mathbf{x}_v^i)]^\lambda. \quad (9)$$

By jointly optimizing the calibration objective in Eq. (9), we can attain an optimal temperature T^* for transferable calibration, along with a task-specific optimal λ^* for bias reduction. [51] also introduced a control value to importance weighting for model selection, but it was used as a hyperparameter. This work further makes itself learnable in a unified hyperparameter-free optimization framework.

3.4 Variance Reduction by Serial Control Variate

Through the above analysis, we enable transferable calibration and further reduce its bias. However, another main drawback of importance weighting is uncontrolled *variance* as the importance weighted estimator can be drastically exploded by a few bad samples with large weights. For simplicity, we denote $w(\mathbf{x}) \mathcal{L}_{\text{ECE}}(\phi(\mathbf{x}), \mathbf{y})$ as $\mathcal{L}_{\text{ECE}}^w$. Replacing the estimated target error from Lemma 2 of [9] with $\mathcal{L}_{\text{ECE}}^w$, we can conclude that the variance of transferable calibration error can be bounded by Rényi divergence between p and q (A proof is provided in B.1 of Appendix):

$$\begin{aligned} \text{Var}_{\mathbf{x} \sim p} [\mathcal{L}_{\text{ECE}}^w] &= \mathbb{E}_{\mathbf{x} \sim p} [(\mathcal{L}_{\text{ECE}}^w)^2] - (\mathbb{E}_{\mathbf{x} \sim p} [\mathcal{L}_{\text{ECE}}^w])^2 \\ &\leq d_{\alpha+1}(q||p)(\mathbb{E}_{\mathbf{x} \sim p} \mathcal{L}_{\text{ECE}}^w)^{1-\frac{1}{\alpha}} - (\mathbb{E}_{\mathbf{x} \sim p} \mathcal{L}_{\text{ECE}}^w)^2, \quad \forall \alpha > 0. \end{aligned} \quad (10)$$

Apparently, lowering the variance of $\mathcal{L}_{\text{ECE}}^w$ results in more accurate estimation. First, Rényi divergence [47] between p and q can be reduced by deep domain adaptation methods [31, 15, 64]. Second, developing bias reduction term in 3.3 may unexpectedly increase the estimation variance, thus we further reduce the variance via the *parameter-free* control variate method [27]. It introduces a related unbiased estimator t to the estimator u that we concern, achieving a new estimator $u^* = u + \eta(t - \tau)$ while $\mathbb{E}[t] = \tau$. As proved in A.3 of Appendix, $\text{Var}[u^*] \leq \text{Var}[u]$ is held and u^* has an optimal solution when $\hat{\eta} = -\text{Cov}(u, t)/\text{Var}[t]$. For brevity, denote $\mathbb{E}_q(\hat{\mathbf{y}}, \mathbf{y}) = \mathbb{E}_{\mathbf{x} \sim p} [\tilde{w}(\mathbf{x}) \mathcal{L}_{\text{ECE}}(\phi(\mathbf{x}), \mathbf{y})]$ as $\mathbb{E}_{\mathbf{x} \sim p} \mathcal{L}_{\text{ECE}}^{\tilde{w}}$ hereafter. To reduce $\text{Var}_{\mathbf{x} \sim p} [\mathcal{L}_{\text{ECE}}^{\tilde{w}}]$, we first adopt the importance weight $\tilde{w}(\mathbf{x})$ as the control variate since the expectation of $\tilde{w}(\mathbf{x})$ is approximately fixed: $\mathbb{E}_{\mathbf{x} \sim p} [\tilde{w}(\mathbf{x})] = 1$. Here, regard $\mathbb{E}_{\mathbf{x} \sim p} [\mathcal{L}_{\text{ECE}}^{\tilde{w}}]$ and $\tilde{w}(\mathbf{x})$ as u and t respectively, and we can attain a new unbiased estimator. When η achieves the optimal solution, the estimation of target calibration error with control variate is

$$\mathbb{E}_q^*(\hat{\mathbf{y}}, \mathbf{y}) = \tilde{\mathbb{E}}_q(\hat{\mathbf{y}}, \mathbf{y}) - \frac{1}{n_s} \frac{\text{Cov}(\mathcal{L}_{\text{ECE}}^{\tilde{w}}, \tilde{w}(\mathbf{x}))}{\text{Var}[\tilde{w}(\mathbf{x})]} \sum_{i=1}^{n_s} [\tilde{w}(\mathbf{x}_s^i) - 1]. \quad (11)$$

Further, we can add the prediction correctness on the source domain $r(\mathbf{x}) = \mathbf{1}(\hat{\mathbf{y}} = \mathbf{y})$ as another control variate because its expectation is also fixed: $\mathbb{E}_{\mathbf{x} \sim p} [r(\mathbf{x})] = c$, *i.e.*, the accuracy should be equal to the confidence c on a perfect calibrated source model as defined in Section 3.1. In this way, control variate method can be easily extended into the serial version in which there is a collection of control variables: t_1, t_2 whose corresponding expectations are τ_1, τ_2 respectively. Formally,

$$\begin{aligned} u^* &= u + \eta_1(t_1 - \tau_1), \\ u^{**} &= u^* + \eta_2(t_2 - \tau_2). \end{aligned} \quad (12)$$

Plugging $r(\mathbf{x})$ as the second control variate into the bottom line of Eq. (12), we can further reduce the variance of target calibration error by the serial control variate method as

$$\mathbb{E}_q^{**}(\hat{\mathbf{y}}, \mathbf{y}) = \mathbb{E}_q^*(\hat{\mathbf{y}}, \mathbf{y}) - \frac{1}{n_s} \frac{\text{Cov}(\mathcal{L}_{\text{ECE}}^{\tilde{w}^*}, r(\mathbf{x}))}{\text{Var}[r(\mathbf{x})]} \sum_{i=1}^{n_s} [r(\mathbf{x}_s^i) - c], \quad (13)$$

where $\mathcal{L}_{\text{ECE}}^{\tilde{w}^*}$ is the estimated target calibration error after applying the control variate to weight $\tilde{w}(\mathbf{x})$. Similarly, replacing the $\mathbb{E}_{\mathbf{x} \sim p} \mathcal{L}_{\text{ECE}}^{\tilde{w}}$ defined in Eq. 9 with $\mathbb{E}_q^{**}(\hat{\mathbf{y}}, \mathbf{y})$ defined in Eq. 13 and then optimizing the new objective, we can attain a more accurate calibration with lower bias and variance.

Algorithm 1 Transferable Calibration in Domain Adaptation

- 1: **Input:** Labeled source dataset $\mathcal{S} = \{(\mathbf{x}_s^i, \mathbf{y}_s^i)\}_{i=1}^{n_s}$ and unlabeled target dataset $\mathcal{T} = \{(\mathbf{x}_t^i)\}_{i=1}^{n_t}$
 - 2: **Parameter:** Temperature T and learnable meta parameter λ
 - 3: Partition \mathcal{S} into $\mathcal{S}_{tr} = \{(\mathbf{x}_{tr}^i, \mathbf{y}_{tr}^i)\}_{i=1}^{n_{tr}}$ and $\mathcal{S}_v = \{(\mathbf{x}_v^i, \mathbf{y}_v^i)\}_{i=1}^{n_v}$
 - 4: Train a DA model $\phi(\mathbf{x}) = G(F(\mathbf{x}))$ on \mathcal{S}_{tr} and \mathcal{T} via any DA method until convergy
 - 5: Randomly upsample the source or the target dataset to make $n_{tr} = n_t$
 - 6: Fix the DA model and compute features $\mathcal{F}_{tr} = \{\mathbf{f}_{tr}^i\}_{i=1}^{n_{tr}}$, $\mathcal{F}_v = \{\mathbf{f}_v^i\}_{i=1}^{n_v}$, $\mathcal{F}_t = \{\mathbf{f}_t^i\}_{i=1}^{n_t}$
 - 7: Train a logistic regression model H to discriminate the features \mathcal{F}_{tr} and \mathcal{F}_t until converge
 - 8: Compute $\hat{w}(\mathbf{x}_v^i) = [1 - H(\mathbf{f}_v^i)] / H(\mathbf{f}_v^i)$ and $\tilde{w}(\mathbf{x}_v^i) = [\hat{w}(\mathbf{x}_v^i)]^\lambda$
 - 9: Compute $\mathbb{E}_{\mathbf{x} \sim p} \mathcal{L}_{ECE}^{\tilde{w}}$, $\mathbb{E}_q^*(\hat{\mathbf{y}}, \mathbf{y})$ and $\mathbb{E}_q^{**}(\hat{\mathbf{y}}, \mathbf{y})$ as in Eq. 9, Eq. 11 and Eq. 13 respectively
 - 10: Jointly optimize the transferable calibration objective as $T^* = \arg \min_{T, \lambda} \mathbb{E}_q^{**}(\sigma(\phi(\mathbf{x}_v)/T), \mathbf{y}_v)$
 - 11: Calibrate the logit vectors on the target domain by $\hat{\mathbf{y}}_t = \sigma(\phi(\mathbf{x}_t)/T^*)$
-

In summary, the transferable calibration framework (3)–(4) is improved through: 1) *lowering bias* as (9); 2) *lowering variance* by deep adaptation as (10) and by serial control variate as (11) and (13). The overall process of TransCal is summarized in Algorithm 1. Integrating the above explanation, TransCal is designed to achieve more accurate calibration in domain adaptation with lower bias and variance in a unified hyperparameter-free optimization framework.

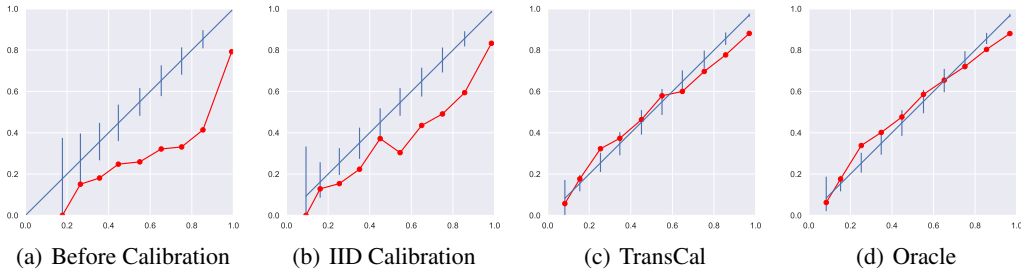


Figure 2: Reliability diagrams from *Clipart* to *Product* with CDAN [31] before and after calibration.

4 Experiments

4.1 Setup

We fully verify our methods on six DA datasets: (1) *Office-Home* [54]: a dataset with 65 categories, consisting of 4 domains: *Artistic (A)*, *Clipart (C)*, *Product (P)* and *Real-World (R)*. (2) *VisDA-2017* [42], a Simulation-to-Real dataset with 12 categories. (3) *ImageNet-Sketch* [55], a large-scale dataset transferring from ImageNet (I) to Sketch (S) with 1000 categories. (4) *Multi-Domain Sentiment* [4], a NLP dataset, comprising of product reviews from *amazon.com* in four product domains: books (B), dvds (D), electronics (E), and kitchen appliances (K). (5) *DomainNet* [41]: a dataset with 345 categories, including 6 domains: *Infograph (I)*, *Quickdraw (Q)*, *Real (R)*, *Sketch (S)*, *Clipart (C)* and *Painting (P)*. (6) *Office-31* [48] contains 31 categories from 3 domains: *Amazon (A)*, *Webcam (W)*, *DSLr (D)*. We run each experiment for 10 times. We denote *Vanilla* as the standard softmax method before calibration, *Oracle* as the temperature scaling method while the target labels are available. Detailed descriptions are included in C.1, C.2 and C.3 of *Appendix*.

4.2 Results

Qualitative Results. As shown in Figure 2, the blue lines indicate the distributions for *perfectly* reliable forecasts with standard deviation, and the red lines denote the conditional distributions of the observations. Obviously, If the model is perfectly calibrated, these two lines should be matched. We

Table 2: ECE (%) vs. Acc (%) via various calibration methods on *Office-Home* with CDAN

Metric	Cal. Method	A→C	A→P	A→R	C→A	C→P	C→R	R→A	R→C	R→P	Avg
Acc	Before Cal.	49.4	68.4	75.5	57.6	70.1	70.4	68.9	54.4	81.2	68.3
	MC-dropout [13]	47.2	66.2	71.4	57.1	65.7	70.6	68.3	53.6	80.7	66.7
	TransCal (ours)	49.4	68.4	75.5	57.6	70.1	70.4	68.9	54.4	81.2	68.3
ECE	Before Cal.	40.2	26.4	17.8	35.8	23.5	21.9	24.8	36.4	14.5	26.8
	MC-dropout [13]	33.1	21.3	15.0	24.2	20.5	13.2	25.6	14.2	22.4	19.6
	Matrix Scaling	44.7	28.8	19.7	36.1	25.4	24.1	38.1	15.7	29.5	29.1
	Vector Scaling	34.7	18.0	11.3	23.4	15.4	11.5	27.3	8.5	20.0	18.9
	Temp. Scaling	28.3	17.6	10.1	21.2	<u>13.2</u>	8.2	26.0	8.8	18.1	16.8
	CPCS [39]	35.0	29.4	8.3	<u>21.3</u>	29.0	5.6	19.9	9.1	20.3	19.8
	TransCal (w/o Bias)	21.7	<u>10.8</u>	<u>5.8</u>	27.6	9.2	<u>6.0</u>	27.4	5.2	<u>16.9</u>	<u>14.5</u>
TransCal (w/o Variance)	31.2	16.4	6.5	31.1	14.7	16.1	27.5	4.1	20.0	18.6	
TransCal (ours)	<u>22.9</u>	9.3	5.1	21.7	14.0	6.4	<u>21.6</u>	<u>4.5</u>	15.6	13.5	
Oracle		5.8	8.1	4.8	10.0	7.7	4.2	5.5	3.9	6.2	6.2

Table 3: ECE (%) before and after various calibration methods on several DA methods and datasets.

Method	Dataset	<i>Office-Home</i>							<i>Sketch</i>	<i>VisDA</i>
	Transfer Task	A→C	A→P	A→R	C→A	C→P	C→R	Avg	I→S	S→R
MDD	Before Cal. (Vanilla)	33.6	18.7	13.0	28.9	22.9	19.0	22.7	19.7	30.5
	IID Cal. (Temp. Scaling)	28.7	16.4	9.3	21.8	16.5	12.1	17.5	14.7	29.1
	CPCS [39]	29.5	17.3	9.6	22.9	16.7	11.8	18.0	14.2	30.4
	TransCal (ours)	13.5	11.4	4.8	21.8	7.0	11.1	11.6	8.1	16.1
	Oracle	6.8	8.5	4.7	7.0	5.8	4.0	6.1	4.7	7.4
MCD	Before Cal. (Vanilla)	39.4	28.8	20.5	33.9	27.9	20.1	28.4	18.3	25.7
	IID Cal. (Temp. Scaling)	21.8	22.0	15.1	22.5	20.5	9.1	18.5	13.0	23.2
	CPCS [39]	23.1	22.3	15.4	20.6	20.0	9.0	18.4	12.9	22.9
	TransCal (ours)	13.1	20.2	5.1	15.5	9.3	9.1	12.0	10.2	7.8
	Oracle	5.6	9.4	2.3	7.1	7.4	2.5	5.7	3.6	1.8

can see that TransCal is much better and approaches the *Oracle* one on the task: Clipart → Product. More reliability diagrams of other tasks to back up this conclusion are shown in [D.3](#) of *Appendix*.

Quantitative Results. As reported in [Table 2](#) and [Table 3](#), TransCal achieves much lower ECE than competitors (decreases about 30% or more, e.g. when TransCal is used to calibrate MCD on VisDA, the target ECE is reduced from 22.9 to 7.8) on various datasets and domain adaptation methods. Some results of TransCal are even approaching the Oracle ones. Further, the ablation studies on *TransCal (w/o Bias)* and *TransCal (w/o Variance)* verify that both bias reduction term and variance reduction term are effective. TransCal can be generalized to other tasks of Office-Home ([D.2.1](#)), to more DA methods ([D.2.2](#)), and to DomainNet and Office-31 ([D.2.3](#)), all shown in *Appendix*. Further, the results evaluated by NLL and BS metrics are included in [D.2.4](#) and [D.2.5](#) of *Appendix* respectively. Apart from computer vision datasets, TransCal performs well in 12 transfer tasks of a popular NLP dataset: *Amazon Multi-Domain Sentiment* in [Table 4](#). As shown in [Table 2](#), it is noteworthy that TransCal

Table 4: ECE (%) via various calibration methods on *Multi-Domain Sentiment*.

Cal. Method	B→D	B→E	B→K	D→B	D→E	D→K	E→B	E→D	E→K	K→B	K→D	K→E	Avg
Before Cal.	13.7	15.2	17.5	20.4	18.6	21.4	11.3	10.3	23.0	13.1	14.5	20.9	16.7
Temp. Scaling	5.9	8.2	5.0	2.6	5.5	4.0	17.1	17.3	6.2	16.5	14.9	6.6	9.2
TransCal (ours)	8.0	6.1	3.8	2.4	1.4	4.0	7.7	8.4	2.2	10.9	11.2	4.2	5.9
Oracle	2.0	3.0	3.6	1.9	1.3	2.5	2.6	1.4	1.8	2.9	2.0	1.6	2.2

maintains the same accuracy with that before calibration while built-in methods (e.g. MC-dropout) may *degrade* prediction accuracy, and they have to modify the network architecture (e.g. adding dropout layers). We further show that both Vector Scaling and Matrix Scaling underperform TransCal and Temp Scaling. Matrix Scaling works even worse than the Vanilla model due to overfitting, which was also observed in the results of Guo *et al.* [21] reported in Table 2.

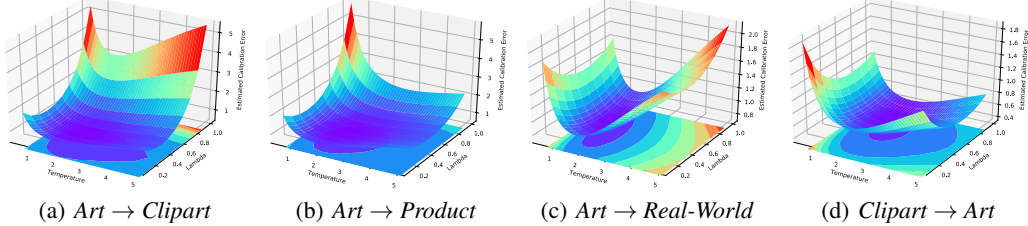


Figure 3: The estimated calibration error with respect to different values of temperature T and meta parameter λ (both are *learnable*), showing that different models achieve optimal values at different λ .

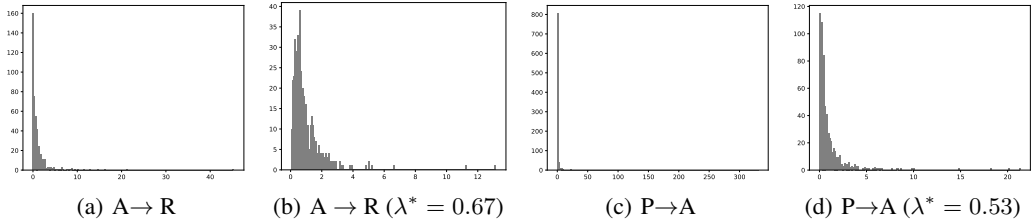


Figure 4: Importance weight distribution of two DA tasks after transferable calibration with (4(b), 4(d)) and without (4(a), 4(c)) applying the learnable meta parameter, which lowers the value of M .

Table 5: ECE (%) of TransCal with different control variate (CV) methods on MDD [64].

Dataset	Office-Home			Sketch	VisDA
	A→C	A→P	A→R	I→S	S→R
Transfer Task					
TransCal (w/o Control Variate)	20.9±4.68	12.1±2.46	6.8±2.22	9.7±3.17	17.2±5.74
TransCal (CV via only $w(\mathbf{x})$)	13.9±4.45	9.6 ±1.52	5.9±1.91	9.3±1.68	16.4±5.68
TransCal (CV via only $r(\mathbf{x})$)	13.8±4.32	10.2±0.97	5.2±1.08	8.6±1.37	16.3±3.32
TransCal (Parallel Control Variate)	13.6±4.43	10.6±1.46	5.2±1.45	8.7±1.54	16.3±3.45
TransCal (Serial Control Variate)	13.5±3.51	11.4± 0.81	4.8±0.76	8.1±1.09	16.1±1.20

4.3 Insight Analyses

Why Bias Reduction Term Works. From the perspective of optimization, we explore the estimated calibration error with respect to different values of temperature (T) and lambda (λ) in Figure 3, showing that different models achieve optimal values at different λ . Thus, it is impossible to attain optimal estimated calibration error by presetting a fixed λ . However, with our unified meta-parameter optimization framework, we can adaptively find an optimal λ for each task. From the perspective of importance weight distribution as shown in Figure 4, after applying learnable meta parameter λ , the highest values (M in Section 3.3) of importance weight decrease, leading to a smaller bias in Eq. (5).

Why Serial Control Variate Works. As the theoretical analysis in B.2 of Appendix shows, the variance of \mathbb{E}_q^{**} can be further reduced since $\text{Var}[\mathbb{E}_q^{**}] \leq \text{Var}[\mathbb{E}_q^*] \leq \text{Var}[\tilde{\mathbb{E}}_q]$, but other variants of control variate (CV) method such as Parallel CV may not hold this property. Meanwhile, as shown in Table 5, TransCal (Serial CV) not only achieves better calibration performance but also attains lower calibration variance than other variants of control variate methods.

5 Conclusion

In this paper, we delve into an open and important problem of *Calibration in DA*. We first reveal that domain adaptation models learn higher accuracy *at the expense of* well-calibrated probabilities. Further, we propose a novel transferable calibration (TransCal) approach, achieving more accurate calibration with lower bias and variance in a unified hyperparameter-free optimization framework.

Broader Impact

The open problem of *Calibration in DA* that we delve into is a very promising research direction and important for decision making in safety-critical applications, such as automated diagnosis system for lung cancer. Since our method can be easily applied to recalibrate the existing DA methods and generate more reliable predictions, it will benefit the transfer learning community. If the method fails in some extreme circumstances, it will confuse researchers or engineers who apply our method but it will not bring about any negative ethical or societal consequences. Meanwhile, our method did not leverage biases in the data such as racial discrimination and gender discrimination since we conduct experiments on standard domain adaptation datasets that are more about animals or pieces of equipment in the office. In summary, we hold a positive view of the broader impact on this paper.

Acknowledgements

This work was supported by the National Natural Science Foundation of China (61772299, 71690231), Beijing Nova Program (Z201100006820041), University S&T Innovation Plan by the Ministry of Education of China.

References

- [1] M. A. Alexandari, A. Kundaje, and A. Shrikumar. Maximum likelihood with bias-corrected calibration is hard-to-beat at label shift adaptation. *ICML*, 2020.
- [2] K. Azizzadenesheli, A. Liu, F. Yang, and A. Anandkumar. Regularized learning for domain adaptation under label shifts. In *ICLR*, 2019.
- [3] S. Bickel and T. Scheffer. Dirichlet-enhanced spam filtering based on biased samples. In *NeurIPS*. MIT Press, 2007.
- [4] J. Blitzer, M. Dredze, and F. Pereira. Biographies, bollywood, boom-boxes and blenders: Domain adaptation for sentiment classification. In *ACL*, 2007.
- [5] C. Blundell, J. Cornebise, K. Kavukcuoglu, and D. Wierstra. Weight uncertainty in neural network. In *ICML*, 2015.
- [6] G. W. BRIER. Verification of forecasts expressed in terms of probability. *Monthly Weather Review*, 78(1):1–3, 1950.
- [7] J. Q. Candela, C. E. Rasmussen, F. H. Sinz, O. Bousquet, and B. Schölkopf. Evaluating predictive uncertainty challenge. In *Machine Learning Challenges*, 2005.
- [8] K. F. Cheng and C. K. Chu. Semiparametric density estimation under a two-sample density ratio model. *Bernoulli*, 10(4):583–604, 2004.
- [9] C. Cortes, Y. Mansour, and M. Mohri. Learning bounds for importance weighting. In *Advances in Neural Information Processing Systems 23*, pages 442–450. Curran Associates, Inc., 2010.
- [10] S. Cui, S. Wang, J. Zhuo, L. Li, Q. Huang, and Q. Tian. Towards discriminability and diversity: Batch nuclear-norm maximization under label insufficient situations. In *CVPR*, June 2020.
- [11] M. H. DeGroot and S. E. Fienberg. The comparison and evaluation of forecasters. *Journal of the Royal Statistical Society. Series D (The Statistician)*, 32(1/2):12–22, 1983.
- [12] J. Donahue, Y. Jia, O. Vinyals, J. Hoffman, N. Zhang, E. Tzeng, and T. Darrell. Decaf: A deep convolutional activation feature for generic visual recognition. In *ICML*, 2014.
- [13] Y. Gal and Z. Ghahramani. Dropout as a bayesian approximation: Representing model uncertainty in deep learning. In *ICML*, 2016.

- [14] Y. Ganin and V. Lempitsky. Unsupervised domain adaptation by backpropagation. In *ICML*, 2015.
- [15] Y. Ganin, E. Ustinova, H. Ajakan, P. Germain, H. Larochelle, F. Laviolette, M. Marchand, and V. Lempitsky. Domain-adversarial training of neural networks. *JMLR*, 2016.
- [16] B. Gong, K. Grauman, and F. Sha. Connecting the dots with landmarks: Discriminatively learning domain-invariant features for unsupervised domain adaptation. In *ICML*, 2013.
- [17] B. Gong, Y. Shi, F. Sha, and K. Grauman. Geodesic flow kernel for unsupervised domain adaptation. In *CVPR*, 2012.
- [18] I. Goodfellow, J. Pouget-Abadie, M. Mirza, B. Xu, D. Warde-Farley, S. Ozair, A. Courville, and Y. Bengio. Generative adversarial nets. In *NeurIPS*, 2014.
- [19] I. J. Goodfellow, Y. Bengio, and A. C. Courville. *Deep Learning*. Adaptive computation and machine learning. MIT Press, 2016.
- [20] A. Gretton, D. Sejdinovic, H. Strathmann, S. Balakrishnan, M. Pontil, K. Fukumizu, and B. K. Sriperumbudur. Optimal kernel choice for large-scale two-sample tests. In *NeurIPS*, 2012.
- [21] C. Guo, G. Pleiss, Y. Sun, and K. Q. Weinberger. On calibration of modern neural networks. In *ICML*, 2017.
- [22] T. Hastie, R. Tibshirani, and J. H. Friedman. *The Elements of Statistical Learning: Data Mining, Inference, and Prediction, 2nd Edition*. Springer Series in Statistics. Springer, 2009.
- [23] K. He, X. Zhang, S. Ren, and J. Sun. Deep residual learning for image recognition. In *CVPR*, 2016.
- [24] J. Huang, A. J. Smola, A. Gretton, K. M. Borgwardt, and B. Schölkopf. Correcting sample selection bias by unlabeled data. In *NeurIPS*, 2006.
- [25] A. Kumar, P. Liang, and T. Ma. Verified uncertainty calibration. In *NeurIPS*, 2019.
- [26] B. Lakshminarayanan, A. Pritzel, and C. Blundell. Simple and scalable predictive uncertainty estimation using deep ensembles. In *NeurIPS*, 2017.
- [27] C. Lemieux. Control variates. In *Wiley StatsRef: Statistics Reference Online*, pages 1–8. American Cancer Society, 2017.
- [28] Z. C. Lipton, Y. Wang, and A. J. Smola. Detecting and correcting for label shift with black box predictors. In *ICML*, 2018.
- [29] M. Long, Y. Cao, Z. Cao, J. Wang, and M. I. Jordan. Transferable representation learning with deep adaptation networks. *TPAMI*, 2018.
- [30] M. Long, Y. Cao, J. Wang, and M. I. Jordan. Learning transferable features with deep adaptation networks. In *ICML*, 2015.
- [31] M. Long, Z. Cao, J. Wang, and M. I. Jordan. Conditional adversarial domain adaptation. In *NeurIPS*, 2018.
- [32] M. Long, H. Zhu, J. Wang, and M. I. Jordan. Unsupervised domain adaptation with residual transfer networks. In *NeurIPS*, 2016.
- [33] M. Long, H. Zhu, J. Wang, and M. I. Jordan. Deep transfer learning with joint adaptation networks. In *ICML*, 2017.
- [34] C. Louizos and M. Welling. Multiplicative normalizing flows for variational bayesian neural networks. In *ICML*, 2017.

- [35] M. P. Naeni, G. F. Cooper, and M. Hauskrecht. Obtaining well calibrated probabilities using bayesian binning. In *AAAI*, 2015.
- [36] M. Oquab, L. Bottou, I. Laptev, and J. Sivic. Learning and transferring mid-level image representations using convolutional neural networks. In *CVPR*, 2014.
- [37] Y. Ovadia, E. Fertig, and J. Ren. Can you trust your model’s uncertainty? evaluating predictive uncertainty under dataset shift. In *NeurIPS*, 2019.
- [38] S. J. Pan and Q. Yang. A survey on transfer learning. *TKDE*, 22(10):1345–1359, 2010.
- [39] S. Park, O. Bastani, J. Weimer, and I. Lee. Calibrated prediction with covariate shift via unsupervised domain adaptation. *AISTATS*, 2020.
- [40] Z. Pei, Z. Cao, M. Long, and J. Wang. Multi-adversarial domain adaptation. In *AAAI*, 2018.
- [41] X. Peng, Q. Bai, X. Xia, Z. Huang, K. Saenko, and B. Wang. Moment matching for multi-source domain adaptation. *ICCV*, 2019.
- [42] X. Peng, B. Usman, N. Kaushik, J. Hoffman, D. Wang, and K. Saenko. Visda: The visual domain adaptation challenge. *CoRR*, abs/1710.06924, 2017.
- [43] J. C. Platt. Probabilistic outputs for support vector machines and comparisons to regularized likelihood methods. In *Advances in Linear Large Margin Classifiers*. MIT Press, 1999.
- [44] J. Qin. Inferences for case-control and semiparametric two-sample density ratio models. *Biometrika*, 85(3):619–630, 1998.
- [45] J. Quionero-Candela, M. Sugiyama, A. Schwaighofer, and N. D. Lawrence. *Dataset Shift in Machine Learning*. The MIT Press, 2009.
- [46] O. Russakovsky, J. Deng, H. Su, J. Krause, S. Satheesh, S. Ma, Z. Huang, A. Karpathy, A. Khosla, M. Bernstein, A. C. Berg, and L. Fei-Fei. ImageNet Large Scale Visual Recognition Challenge. *arXiv:1409.0575*, 2014.
- [47] A. Rényi. On measures of information and entropy. *Proceedings of the 4th Berkeley Symposium on Mathematics, Statistics and Probability*, 1961.
- [48] K. Saenko, B. Kulis, M. Fritz, and T. Darrell. Adapting visual category models to new domains. In *ECCV*, 2010.
- [49] K. Saito, K. Watanabe, Y. Ushiku, and T. Harada. Maximum classifier discrepancy for unsupervised domain adaptation. In *CVPR*, 2018.
- [50] N. Srivastava, G. E. Hinton, A. Krizhevsky, I. Sutskever, and R. Salakhutdinov. Dropout: a simple way to prevent neural networks from overfitting. *J. Mach. Learn. Res.*, 2014.
- [51] M. Sugiyama, M. Krauledat, and K.-R. Mäzler. Covariate shift adaptation by importance weighted cross validation. *JMLR*, 8:985–1005, 2007.
- [52] E. Tzeng, J. Hoffman, K. Saenko, and T. Darrell. Adversarial discriminative domain adaptation. In *CVPR*, 2017.
- [53] E. Tzeng, J. Hoffman, N. Zhang, K. Saenko, and T. Darrell. Deep domain confusion: Maximizing for domain invariance. *CoRR*, abs/1412.3474, 2014.
- [54] H. Venkateswara, J. Eusebio, S. Chakraborty, and S. Panchanathan. Deep Hashing Network for Unsupervised Domain Adaptation. In *CVPR*, 2017.
- [55] H. Wang, S. Ge, E. P. Xing, and Z. C. Lipton. Learning robust global representations by penalizing local predictive power. *NeurIPS*, 2019.

- [56] X. Wang, Y. Jin, M. Long, J. Wang, and M. I. Jordan. Transferable normalization: Towards improving transferability of deep neural networks. In *NeurIPS*, 2019.
- [57] X. Wang, L. Li, W. Ye, M. Long, and J. Wang. Transferable attention for domain adaptation. In *AAAI*, 2019.
- [58] Y. Wen, P. Vicol, J. Ba, D. Tran, and R. B. Grosse. Flipout: Efficient pseudo-independent weight perturbations on mini-batches. In *ICLR*, 2018.
- [59] R. Xu, G. Li, J. Yang, and L. Lin. Unsupervised domain adaptation: An adaptive feature norm approach. *ICCV*, 2019.
- [60] J. Yosinski, J. Clune, Y. Bengio, and H. Lipson. How transferable are features in deep neural networks? In *NeurIPS*, 2014.
- [61] K. You, X. Wang, M. Long, and M. Jordan. Towards accurate model selection in deep unsupervised domain adaptation. In *ICML*, 2019.
- [62] B. Zadrozny and C. Elkan. Obtaining calibrated probability estimates from decision trees and naive bayesian classifiers. In *ICML*, 2001.
- [63] B. Zadrozny and C. Elkan. Transforming classifier scores into accurate multiclass probability estimates. In *KDD*, 2002.
- [64] Y. Zhang, T. Liu, M. Long, and M. Jordan. Bridging theory and algorithm for domain adaptation. In *ICML*, 2019.
- [65] H. Zhao, R. T. des Combes, K. Zhang, and G. J. Gordon. On learning invariant representation for domain adaptation. In *ICML*, 2019.

Appendix

In this appendix, we will show more explanations, details, and results that are not included in the main paper. In Preliminaries A, we especially add more detailed formal denifitions of calibration metrics, Rényi Divergence, and control variate method. In Proof B, both the bound for the variance of estimated calibration error and the variance reduction analysis for variants of control variate methods are provided. In Seup C, we provide a detailed description of the experiment setting. In the last section D, more qualitative and quantitative results of TransCal are shown when it is evaluated on other domain adaptation tasks of Office-Home, on more domain adaptation methods, on more domain adaptation datasets (*Office-31* and *DomainNet*), and on NLL and BS.

A Preliminaries

A.1 Calibration Metrics.

Given a deep neural model ϕ (parameterized by θ) which transforms the random variable input X into the class prediction \hat{Y} and its associated confidence \hat{P} , we can define the *perfect calibration* [21] as $\mathbb{P}(\hat{Y} = Y | \hat{P} = c) = c, \forall c \in [0, 1]$ where Y is the ground truth label. As it is impossible to achieve perfect calibration in practical, there are some typical metrics to measure calibration error: Negative Log-Likelihood (NLL), Brier Score (BS), and Expected Calibration Error (ECE).

Negative Log-Likelihood (NLL) [19], also known as the cross-entropy loss in field of deep learning, serves as a proper scoring rule to measure the quality of a probabilistic model [22]. Denote $p(\hat{\mathbf{y}}_i | \mathbf{x}_i, \theta)$ a predicted probability vector associated with the one-hot encoded ground-truth label \mathbf{y}_i for example \mathbf{x}_i in the dataset, NLL can be defined as

$$\mathcal{L}_{\text{NLL}} = - \sum_{i=1}^n \sum_{k=1}^K \mathbf{y}_i^k \log p(\hat{\mathbf{y}}_i^k | \mathbf{x}_i, \theta), \quad (14)$$

where n is the number of samples and K is the number of classes. NLL achieves minimal if and only if the prediction probability $p(\mathbf{y}|\mathbf{x}, \boldsymbol{\theta})$ recovers the ground-truth label \mathbf{y} , however, it may over-emphasize tail probabilities [7].

Brier Score (BS) [6], defined as the squared error between the prediction probability $p(\mathbf{y}|\mathbf{x}, \boldsymbol{\theta})$ and the ground-truth label \mathbf{y} , is another proper scoring rule for uncertainty measurement. Using the same notation of NLL, Brier Score is formally defined as

$$\mathcal{L}_{\text{BS}} = -\frac{1}{K} \sum_{i=1}^n \sum_{k=1}^K (p(\hat{\mathbf{y}}_i^k | \mathbf{x}_i, \boldsymbol{\theta}) - \mathbf{y}_i^k)^2, \quad (15)$$

For classification, BS can be decomposed into calibration and refinement [11], therefore, it conflates accuracy with calibration, causing it not a optimal metric for calibration in DA.

Expected Calibration Error (ECE) [35, 21] first partitions the interval of probability predictions into B bins where B_m is the indices of samples falling into the m -th bin, and then computes the weighted absolute difference between accuracy and confidence across bins:

$$\mathcal{L}_{\text{ECE}} = \sum_{m=1}^B \frac{|B_m|}{n} |\mathbb{A}(B_m) - \mathbb{C}(B_m)|, \quad (16)$$

where for each bin m , the accuracy is $\mathbb{A}(B_m) = |B_m|^{-1} \sum_{i \in B_m} \mathbf{1}(\hat{\mathbf{y}}_i = \mathbf{y}_i)$ and its confidence is $\mathbb{C}(B_m) = |B_m|^{-1} \sum_{i \in B_m} \max_k p(\hat{\mathbf{y}}_i^k | \mathbf{x}_i, \boldsymbol{\theta})$. ECE is easier to interpret and thereby more popular.

A.2 Rényi Divergence [47]

Akin to [9, 61], our analysis also based on the widely-used notation of Rényi divergence [47], which is an information-theoretical measure directly relevant to the study of importance weighting. Given a hyper-parameter $\alpha \geq 0$ and $\alpha \neq 1$, Rényi divergence between distribution p and q is defined as

$D_\alpha(p||q) = \frac{1}{\alpha-1} \log_2 \sum_x p(x) \left(\frac{p(x)}{q(x)}\right)^{\alpha-1}$. Rényi divergence is well-defined: it is non-negative and $D_\alpha(p||q) = 0$ if and only if $p = q$. Particularly, when $\alpha = 1$, it coincides with Kullback–Leibler divergence, i.e., $\lim_{\alpha \rightarrow 1} D_\alpha(p||q) = KL(p||q)$. Here, another notation of Rényi divergence is adopted:

$$d_\alpha(p||q) = 2^{D_\alpha(p||q)} = \left[\sum_x \frac{p^\alpha(x)}{q^{\alpha-1}(x)} \right]^{\frac{1}{\alpha-1}}. \quad (17)$$

A.3 Control Variate [27]

To reduce variance, an effective technique typically employed in Monte Carlo methods named as *Control Variate* [27] is introduced here. Denote the statistic u an unbiased estimator of an unknown parameter μ , i.e. $\mathbb{E}[u] = \mu$. To reduce its variance, we introduce a related unbiased estimator t such that $\mathbb{E}[t] = \tau$, in which τ is the parameter that t tries to estimate. Then, a new estimator u^* with a constant η can be constructed as

$$u^* = u + \eta(t - \tau). \quad (18)$$

u^* has two important properties: 1) u^* is still an *unbiased* unbiased estimator of μ since $\mathbb{E}[u^*] = \mathbb{E}[u] + \eta\mathbb{E}[t - \tau] = \mu + \eta * (\mathbb{E}[t] - \mathbb{E}[\tau]) = \mu$; 2) The variance $\text{Var}[u^*]$ of u^* is *reduced*, i.e., $\text{Var}[u^*] \leq \text{Var}[u]$. That is because the variance of u^* can be decomposed into

$$\text{Var}[u^*] = \text{Var}[u + \eta(t - \tau)] = \text{Var}[t]\eta^2 + 2\text{Cov}(u, t)\eta + \text{Var}[u], \quad (19)$$

which is a quadratic form of η and has a optimal solution when $\hat{\eta} = -\text{Cov}(u, t)/\text{Var}[t]$, resulting in a optimal value $(1 - \rho(u, t)^2)\text{Var}[u]$ where ρ is the correlation coefficient. Obviously, ρ satisfies $0 \leq |\rho| \leq 1$, leading to a lower variance: $\text{Var}[u^*] \leq \text{Var}[u]$.

B Proof

B.1 The Bound for the Variance of Estimated Calibration Error

In the main paper, we have mentioned that the main drawback of importance weighting is uncontrolled *variance* as the importance weighted estimator can be drastically exploded by a few bad samples

with large weights. For simplicity, we denote $w(\mathbf{x})\mathcal{L}_{\text{ECE}}(\phi(\mathbf{x}), \mathbf{y})$ as $\mathcal{L}_{\text{ECE}}^w$ as in the main paper. Motivated by the Lemma 2 of the learning bounds for importance weighting [9], we show that the variance of transferable calibration error can be bounded by Rényi divergence between p and q . By using Hölder's Inequality, we provide detailed proof here.

$$\begin{aligned}
\text{Var}_{\mathbf{x} \sim p}[\mathcal{L}_{\text{ECE}}^w] &= \mathbb{E}_{\mathbf{x} \sim p}[(\mathcal{L}_{\text{ECE}}^w)^2] - (\mathbb{E}_{\mathbf{x} \sim p}[\mathcal{L}_{\text{ECE}}^w])^2 \\
&= \mathbb{E}_{\mathbf{x} \sim p} \left[(w(\mathbf{x}))^2 (\mathcal{L}_{\text{ECE}}(\phi(\mathbf{x}), \mathbf{y}))^2 \right] - (\mathbb{E}_{\mathbf{x} \sim p}[\mathcal{L}_{\text{ECE}}^w])^2 \\
&= \sum_{\mathbf{x}} p(\mathbf{x}) \left[\frac{q(\mathbf{x})}{p(\mathbf{x})} \right]^2 (\mathcal{L}_{\text{ECE}}(\phi(\mathbf{x}), \mathbf{y}))^2 - (\mathbb{E}_{\mathbf{x} \sim p}[\mathcal{L}_{\text{ECE}}^w])^2 \\
&= \sum_{\mathbf{x}} (q(\mathbf{x}))^{\frac{1}{\alpha}} \left[\frac{q(\mathbf{x})}{p(\mathbf{x})} \right] (q(\mathbf{x}))^{\frac{\alpha-1}{\alpha}} (\mathcal{L}_{\text{ECE}}(\phi(\mathbf{x}), \mathbf{y}))^2 - (\mathbb{E}_{\mathbf{x} \sim p}[\mathcal{L}_{\text{ECE}}^w])^2 \\
&\leq \left[\sum_{\mathbf{x}} q(\mathbf{x}) \left[\frac{q(\mathbf{x})}{p(\mathbf{x})} \right]^\alpha \right]^{\frac{1}{\alpha}} \left[\sum_{\mathbf{x}} q(\mathbf{x}) (\mathcal{L}_{\text{ECE}}(\phi(\mathbf{x}), \mathbf{y}))^{\frac{2\alpha}{\alpha-1}} \right]^{\frac{\alpha-1}{\alpha}} - (\mathbb{E}_{\mathbf{x} \sim p}[\mathcal{L}_{\text{ECE}}^w])^2 \\
&= d_{\alpha+1}(q\|p) \left[\sum_{\mathbf{x}} q(\mathbf{x}) \mathcal{L}_{\text{ECE}}(\phi(\mathbf{x}), \mathbf{y}) (\mathcal{L}_{\text{ECE}}(\phi(\mathbf{x}), \mathbf{y}))^{\frac{\alpha+1}{\alpha-1}} \right]^{\frac{\alpha-1}{\alpha}} - (\mathbb{E}_{\mathbf{x} \sim p}[\mathcal{L}_{\text{ECE}}^w])^2 \\
&\leq d_{\alpha+1}(q\|p) (\mathbb{E}_{\mathbf{x} \sim p} \mathcal{L}_{\text{ECE}}^w)^{1-\frac{1}{\alpha}} \left[\sum_{\mathbf{x}} \mathcal{L}_{\text{ECE}}(\phi(\mathbf{x}), \mathbf{y}) \right]^{1+\frac{1}{\alpha}} - (\mathbb{E}_{\mathbf{x} \sim p}[\mathcal{L}_{\text{ECE}}^w])^2 \\
&\leq d_{\alpha+1}(q\|p) (\mathbb{E}_{\mathbf{x} \sim p} \mathcal{L}_{\text{ECE}}^w)^{1-\frac{1}{\alpha}} - (\mathbb{E}_{\mathbf{x} \sim p} \mathcal{L}_{\text{ECE}}^w)^2, \quad \forall \alpha > 0.
\end{aligned} \tag{20}$$

Apparently, lowering the variance of $\mathcal{L}_{\text{ECE}}^w$ results in a more accurate estimation. First, Rényi divergence [47] between p and q can be reduced by deep domain adaptation methods [31, 15, 64]. Second, we further reduce the variance by the control variate method [27]. As analyzed in the main paper, these two techniques can be utilized to reduce the variance of the transferable calibration error, and the former one has been verified by the previous works. For a fair comparison, we use deep adapted features in all baselines, including the IID Calibration (Temp. Scaling), IID Calibration (Vector Scaling), IID Calibration (Matrix Scaling) and CPCS [39].

B.2 Variance Reduction Analysis for Variants of Control Variate Methods

B.2.1 Single Control Variate

As analyzed in Section A.3, control variate is an effective and mainstream technique to reduce variance. By introducing a related unbiased estimator t to the estimator u that we concern, we can attain a new estimator $u^* = u + \eta(t - \tau)$. Obviously, the variance of u^* is

$$\text{Var}[u^*] = \text{Var}[u + \eta(t - \tau)] = \text{Var}[t]\eta^2 + 2\text{Cov}(u, t)\eta + \text{Var}[u], \tag{21}$$

which is a quadratic form of η and has a optimal solution when $\hat{\eta} = -\text{Cov}(u, t)/\text{Var}[t]$, resulting in a optimal value $(1 - \rho(u, t)^2)\text{Var}[u]$ where ρ is the correlation coefficient. Obviously, ρ satisfies $0 \leq |\rho| \leq 1$, leading to a lower variance: $\text{Var}[u^*] \leq \text{Var}[u]$. For a single control variate method, both *Control Variate via only $w(\mathbf{x})$* as shown in Eq. (22) and *Control Variate via only $r(\mathbf{x})$* as shown in Eq. (23) can reduce the variance of the target estimated calibration error $\text{Var}[u^*] \leq \text{Var}[u]$.

$$\mathbb{E}_q^{(1)}(\hat{\mathbf{y}}, \mathbf{y}) = \tilde{\mathbb{E}}_q(\hat{\mathbf{y}}, \mathbf{y}) - \frac{1}{n_s} \frac{\text{Cov}(\mathcal{L}_{\text{ECE}}^{\tilde{w}}, \tilde{w}(\mathbf{x}))}{\text{Var}[\tilde{w}(\mathbf{x})]} \sum_{i=1}^{n_s} [\tilde{w}(\mathbf{x}_s^i) - 1]. \tag{22}$$

$$\mathbb{E}_q^{(2)}(\hat{\mathbf{y}}, \mathbf{y}) = \tilde{\mathbb{E}}_q(\hat{\mathbf{y}}, \mathbf{y}) - \frac{1}{n_s} \frac{\text{Cov}(\mathcal{L}_{\text{ECE}}^{\tilde{r}}, r(\mathbf{x}))}{\text{Var}[r(\mathbf{x})]} \sum_{i=1}^{n_s} [r(\mathbf{x}_s^i) - c], \tag{23}$$

B.2.2 Parallel Control Variate

For a parallel control variate method, we extend the control variate method into a parallel version in which there is a collection of control variables: t_1, t_2 whose corresponding expectations are τ_1, τ_2

respectively. By introducing these two related estimators into u , a new estimator is attained:

$$u^* = u + \eta_1(t_1 - \tau_1) + \eta_2(t_2 - \tau_2). \quad (24)$$

Similarly, the variance of u^* in the parallel control variate can be decomposed into:

$$\begin{aligned} \text{Var}[u^*] &= \text{Var}[u + \eta_1(t_1 - \tau_1) + \eta_2(t_2 - \tau_2)] \\ &= \text{Var}[u] + \text{Var}[t_1]\eta_1^2 + 2\text{Cov}(u, t_1)\eta_1 \\ &\quad + 2\text{Cov}(t_1, t_2)\eta_1\eta_2 + \text{Var}[t_2]\eta_2^2 + 2\text{Cov}(u, t_2)\eta_2, \end{aligned} \quad (25)$$

which is much more complex than that of the single control variate whose variance is a quadratic form and has an optimal solution. Set the derivative of $\text{Var}[u^*]$ with respect to η_1 and η_2 to zero:

$$\begin{aligned} \text{Var}[t_1]\eta_1 + \text{Cov}(u, t_1) + \text{Cov}(t_1, t_2)\eta_2 &= 0 \\ \text{Var}[t_2]\eta_2 + \text{Cov}(u, t_2) + \text{Cov}(t_1, t_2)\eta_1 &= 0 \end{aligned} \quad (26)$$

we can attain the optimal solutions of η_1 and η_2 corresponding to the optimal value of $\text{Var}[u^*]$:

$$\begin{aligned} \hat{\eta}_1 &= \frac{\text{Cov}(u, t_1)\text{Var}[t_2] - \text{Cov}(u, t_2)\text{Cov}(t_1, t_2)}{\text{Cov}(t_1, t_2)\text{Cov}(t_1, t_2) - \text{Var}[t_1]\text{Var}[t_2]} \\ \hat{\eta}_2 &= \left[\frac{\text{Cov}(u, t_2)\text{Cov}(t_1, t_2) - \text{Cov}(u, t_1)\text{Var}[t_2]}{\text{Cov}(t_1, t_2)\text{Cov}(t_1, t_2) - \text{Var}[t_1]\text{Var}[t_2]} \right] \frac{\text{Var}[t_1]}{\text{Cov}(t_1, t_2)} - \frac{\text{Cov}(u, t_1)}{\text{Cov}(t_1, t_2)} \end{aligned} \quad (27)$$

By plugging $\hat{\eta}_1$ and $\hat{\eta}_2$ into Eq. (25), we can attain the optimal value of $\text{Var}[u^*]$ as $\text{Var}[u] + \text{Res}[t_1, t_2, u]$. However, the property $\text{Var}[u^*] \leq \text{Var}[u]$ is not always true unless we can guarantee that $\text{Res}[t_1, t_2, u] \leq 0$. In this way, the variance of the target estimated calibration error by the parallel control variate method may not be reduced.

B.2.3 Serial Control Variate

As mentioned in the main paper, the control variate method can be easily extended into the serial version in which there is a collection of control variables: t_1, t_2 whose corresponding expectations are τ_1, τ_2 respectively. That is formally defined as

$$\begin{aligned} u^* &= u + \eta_1(t_1 - \tau_1), \\ u^{**} &= u^* + \eta_2(t_2 - \tau_2). \end{aligned} \quad (28)$$

By using the $w(\mathbf{x})$ and $r(\mathbf{x})$ as the first and the second control variate in Eq. (28), we can further reduce the variance of target calibration error by the serial control variate method as

$$\begin{aligned} \mathbb{E}_q^*(\hat{\mathbf{y}}, \mathbf{y}) &= \tilde{\mathbb{E}}_q(\hat{\mathbf{y}}, \mathbf{y}) - \frac{1}{n_s} \frac{\text{Cov}(\mathcal{L}_{\text{ECE}}^{\tilde{w}}, \tilde{w}(\mathbf{x}))}{\text{Var}[\tilde{w}(\mathbf{x})]} \sum_{i=1}^{n_s} [\tilde{w}(\mathbf{x}_s^i) - 1] \\ \mathbb{E}_q^{**}(\hat{\mathbf{y}}, \mathbf{y}) &= \mathbb{E}_q^*(\hat{\mathbf{y}}, \mathbf{y}) - \frac{1}{n_s} \frac{\text{Cov}(\mathcal{L}_{\text{ECE}}^{\tilde{w}^*}, r(\mathbf{x}))}{\text{Var}[r(\mathbf{x})]} \sum_{i=1}^{n_s} [r(\mathbf{x}_s^i) - c]. \end{aligned} \quad (29)$$

In the serial control variate method, the variance $\text{Var}[u^*]$ and $\text{Var}[u^{**}]$ of u^* and u^{**} are

$$\begin{aligned} \text{Var}[u^*] &= \text{Var}[u + \eta_1(t_1 - \tau_1)] = \text{Var}[t_1]\eta_1^2 + 2\text{Cov}(u, t_1)\eta_1 + \text{Var}[u] \\ \text{Var}[u^{**}] &= \text{Var}[u^* + \eta_2(t_2 - \tau_2)] = \text{Var}[t_2]\eta_2^2 + 2\text{Cov}(u^*, t_2)\eta_2 + \text{Var}[u^*]. \end{aligned} \quad (30)$$

Apparently, the property $\text{Var}[\mathbb{E}_q^{**}] \leq \text{Var}[\mathbb{E}_q^*] \leq \text{Var}[\tilde{\mathbb{E}}_q]$ is held since the above two equations in Eq. (30) have optimal solutions when $\hat{\eta}_1 = -\text{Cov}(u, t_1)/\text{Var}[t_1]$ and $\hat{\eta}_2 = -\text{Cov}(u^*, t_2)/\text{Var}[t_2]$, resulting in a lower and lower variance of the target estimated calibration error.

C Setup

C.1 Datasets

We fully verify our methods on six DA datasets: (1) *Office-Home* [54]: a dataset with 65 categories, consisting of 4 domains: *Artistic (A)*, *Clipart (C)*, *Product (P)* and *Real-World (R)*. (2) *VisDA-2017*

[42], a Simulation-to-Real dataset with 12 categories. (3) *ImageNet-Sketch* [55], a large-scale dataset transferring from ImageNet (**I**) to Sketch (**S**) with 1000 categories. (4) *Multi-Domain Sentiment* [4], a NLP dataset, comprising of product reviews from *amazon.com* in four product domains: books (**B**), dvds (**D**), electronics (**E**), and kitchen appliances (**K**). (5) *DomainNet* [41]: a dataset with 345 categories, including 6 domains: *Infograph* (**I**), *Quickdraw* (**Q**), *Real* (**R**), *Sketch* (**S**), *Clipart* (**C**) and *Painting* (**P**). (6) *Office-31* [48] contains 31 categories from 3 domains: *Amazon* (**A**), *Webcam* (**W**), *DSLR* (**D**). For each dataset, we randomly split it and use the *first 80 percent* for training and the *remaining 20 percent* data for validation. We run each experiment for 10 times. We denote *Vanilla* as the standard softmax method before calibration, *Oracle* as the temperature scaling method while the target labels are available. Detailed descriptions are included in [C.1](#), [C.2](#) and [C.3](#) of *Appendix*.

C.2 Implementation Details

Our methods were implemented based on *PyTorch*. The implementation of our paper consists of two main steps: *Generating Features* and *Transferable Calibration*. When generating features, we use ResNet-50 [23] models pre-trained on the ImageNet dataset [46] as the backbone. As a post-hoc calibration method, we fixed the adapted model when recalibrating the accuracy and confidence. As for the Transferable Calibration step, the *scipy.optimize* package was used to solve the constrained optimization problem. Since no hyperparameter was introduced into the method, we can directly attain the results in all experiments. To objectively verify our method, we use three calibration metrics: Negative Log-Likelihood (NLL), Brier Score (BS), and Expected Calibration Error (ECE). Follow the protocol in [21], we set the number of bins $M = 15$ of ECE to measure calibration error. We run each experiment for 10 times for each task.

C.3 Calibration Methods

We denote *Vanilla* as the standard softmax method before calibration, and *Oracle* as the temperature scaling method while the target labels are available. Meanwhile, *IID Cal. (Temp. Scaling)* is the IID calibration via temperature scaling recalibration method applied on the source domain as adopted in [21], *IID Cal. (Platt Scaling)* as the IID calibration via Platt scaling recalibration method adopted in [43]. Further, we report the results of the transferable calibration method *TransCal* that we proposed, and *TransCal* without bias reduction term: *TransCal (w/o Bias)*, as well as *TransCal* without variance reduction term: *TransCal (w/o Variance)*. For a fair comparison, we use deep adapted features in all baselines, including the IID Calibration (Temp. Scaling) and CPCS [39]. We select three mainstream domain adaptation methods: MCD [49], CDAN [31] and MDD [64] in the main paper. To verify that *TransCal* can be generalized to recalibrate domain adaptation models, we further conduct the experiments with the other two mainstream classical domain adaptation methods: DAN [30], JAN [33], and another two latest domain adaptation methods: AFN [59] and BNM [10].

D Results and Analysis

D.1 More Results to Demonstrate the Dilemma Between Accuracy and Calibration

In Section 1 of the main paper, we uncover a dilemma in the open problem of Calibration in DA: existing domain adaptation models learn higher classification accuracy *at the expense of* well-calibrated probabilities by 12 transfer tasks of *Office-Home*. To verify these phenomena in other datasets and tasks, we further include the results of accuracy and calibration on *Office-31* with 4 tasks: *Amazon* \rightarrow *Webcam*, *Amazon* \rightarrow *DSLR*, *DSLR* \rightarrow *Amazon*, *Webcam* \rightarrow *Amazon* since the other two tasks are too simple, and on *ImageNet-Sketch*, a large-scale dataset transferring from *ImageNet* to *Sketch* consisting of 1000 categories. Note that, besides the five mainstream domain adaptation methods that we reported in the main paper, we further conduct the experiments on other two main stream DA methods: DAN [30], JAN [33], and another latest DA methods: AFN [59] and BNM [10]. As shown in Figure 5, the same conclusion about the dilemma between accuracy and calibration can be drawn on other DA datasets and tasks. Meanwhile, we show the detailed results of accuracy and ECE of 12 transfer tasks on *Office-Home* in Figure 6 to precisely back up our observation of the miscalibration between accuracy and confidence after applying domain adaptation methods.

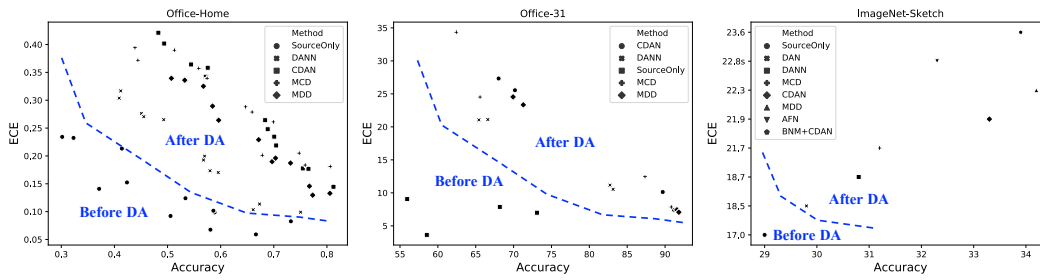


Figure 5: The dilemma between Accuracy and ECE before calibration on more DA methods and datasets (*Office-Home*, *Office-31*, *Sketch*). After applying domain adaptation methods, miscalibration phenomena become severer compared with SourceOnly model, indicating that DA models learn higher accuracy than the SourceOnly ones *at the expense of* well-calibrated probabilities.

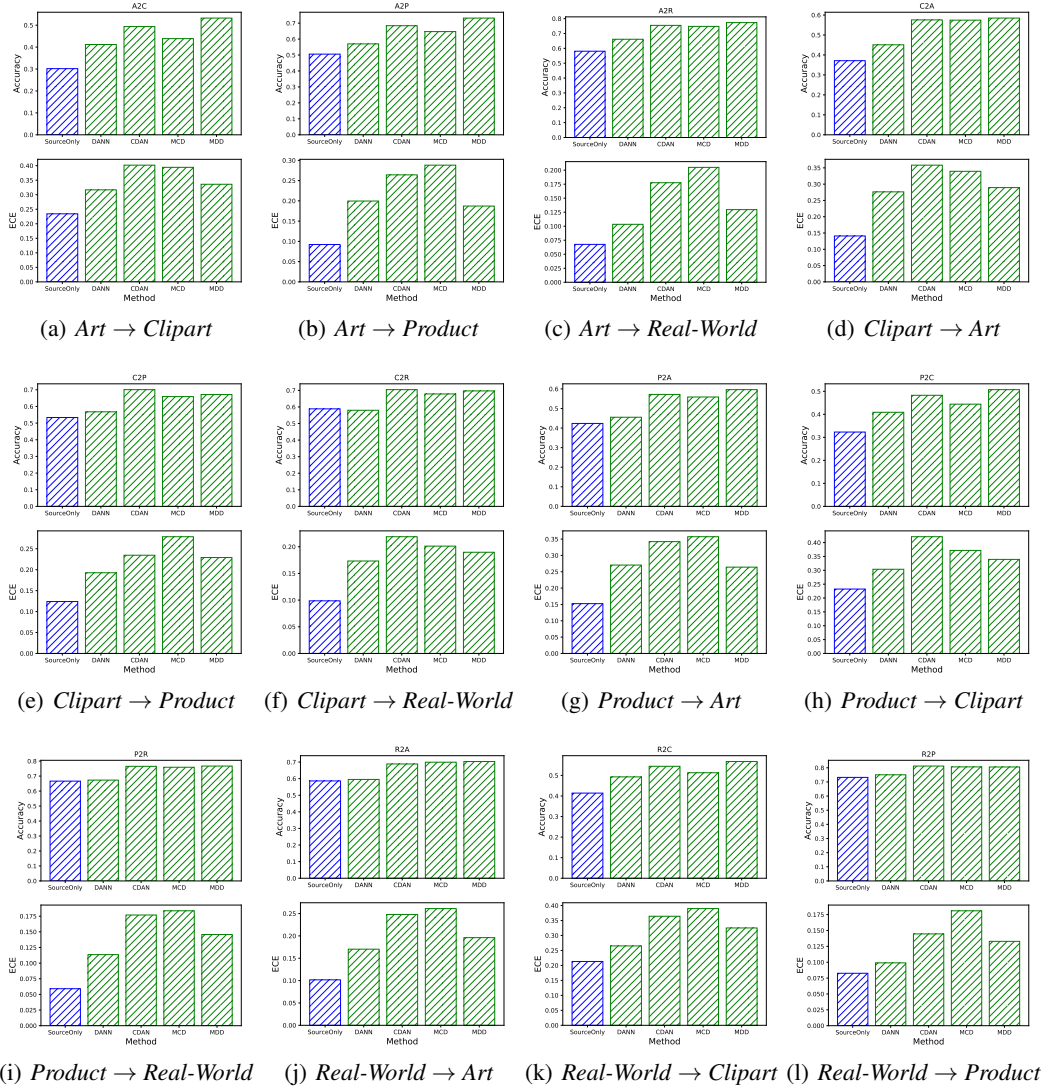


Figure 6: The dilemma between accuracy and ECE for different transfer tasks on *Office-Home*.

D.2 More Quantitative Results

D.2.1 Generalized to Other Tasks of *Office-Home*

Due to the space limit, we only report the first six transfer tasks on *Office-Home* in the main paper, thus we show the calibration results of the other tasks in Table 6. As reported, TransCal also achieves much lower ECE than competitors on other tasks on *Office-Home* while recalibrating various domain adaptation methods. Further, the ablation studies on *TransCal (w/o Bias)* and *TransCal (w/o Variance)* also verify that both bias reduction term and variance reduction term are effective.

Table 6: ECE(%) before and after various calibration methods for other 6 tasks on *Office-Home*.

Method	Transfer Task	P→A	P→C	P→R	R→A	R→C	R→P	Avg
MDD	Before Cal. (Vanilla)	26.4	33.9	14.6	19.6	32.5	13.3	23.4
	IID Cal. (Temp. Scaling)	22.5	30.6	<u>12.1</u>	13.3	26.3	9.8	19.1
	CPCS [39]	24.6	31.6	14.1	13.3	27.0	9.9	20.1
	TransCal (w/o Bias)	25.0	31.8	13.4	<u>10.6</u>	<u>23.2</u>	10.2	19.1
	TransCal (w/o Variance)	21.1	29.5	<u>12.1</u>	<u>12.9</u>	<u>24.0</u>	<u>9.3</u>	<u>18.2</u>
	TransCal (ours)	<u>21.7</u>	<u>30.6</u>	6.5	7.5	23.0	5.6	15.8
Oracle		6.6	6.0	4.7	6.2	6.7	5.2	5.9
MCD	Before Cal. (Vanilla)	35.7	37.2	18.4	26.1	39	18.1	29.1
	IID Cal. (Temp. Scaling)	29.1	28.1	15.9	22.6	31.1	16.3	23.9
	CPCS [39]	30.1	30.4	15.2	21.9	32.8	17.1	24.6
	TransCal (w/o Bias)	<u>19.1</u>	13.7	5.9	19.3	30.7	12.4	16.8
	TransCal (w/o Variance)	20.7	<u>25.5</u>	4.9	7.2	<u>27.9</u>	6.1	<u>15.4</u>
	TransCal (ours)	16.4	27.7	<u>5.5</u>	7.2	23.2	6.1	14.3
Oracle		6.2	4.7	2.6	6.9	8.1	5.3	5.6
CDAN	Before Cal. (Vanilla)	34.2	42.1	17.7	24.8	36.4	14.5	28.3
	IID Cal. (Temp. Scaling)	25.5	32.9	11.5	14.0	26.0	8.8	<u>19.8</u>
	CPCS [39]	27.7	39.2	15.6	13.6	19.9	9.1	20.9
	TransCal (w/o Bias)	26.7	<u>38.8</u>	<u>13.6</u>	<u>10.2</u>	27.4	5.2	20.3
	TransCal (w/o Variance)	<u>22.1</u>	41.7	15.7	13.0	27.5	4.1	20.7
	TransCal (ours)	18.5	40.4	13.9	9.1	<u>21.6</u>	<u>4.5</u>	18.0
Oracle		10.2	4.8	3.8	6.1	5.5	3.9	5.7

D.2.2 Generalized to More Domain Adaptation Methods

To verify that TransCal can be generalized to recalibrate DA methods, we further conduct the experiments with the other two mainstream DA methods: DAN [30], JAN [33], and another latest DA methods: AFN [59] and BNM [10]. As shown in Figure 7, we conduct experiments on *Visda-2017* to recalibrate the above four DA methods. The results demonstrate that TransCal also performs well for these DA methods, resulting in a lower calibration error for each task.

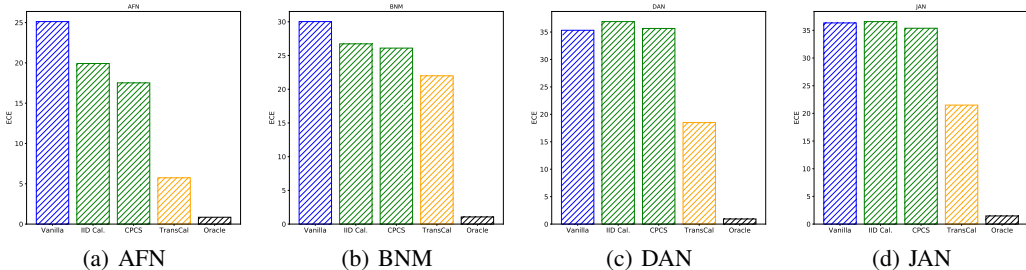


Figure 7: ECE(%) before and after various calibration methods for more DA methods on *Visda*.

D.2.3 Generalized to More Domain Adaptation Datasets

As shown in Figure 8, Figure 9, Figure 10 and Figure 11, TransCal also achieves much lower ECE than competitors on some domain adaptation tasks of *Office-31* and *DomainNet*.

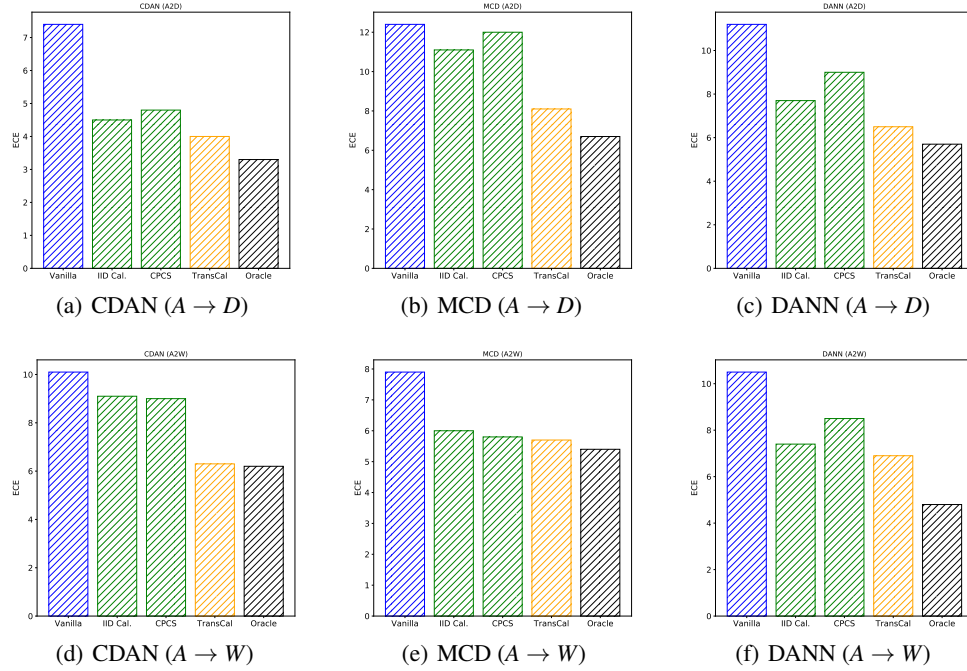


Figure 8: ECE (%) before and after various calibration methods for several DA methods on *Office-31*.

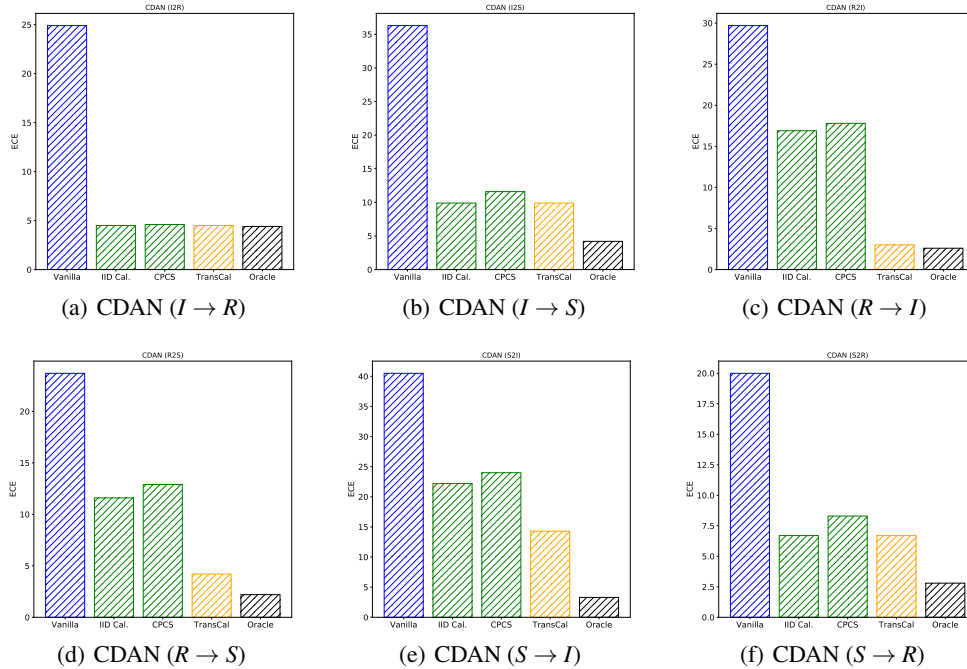


Figure 9: ECE(%) before and after various calibration methods for CDAN on *DomainNet*.

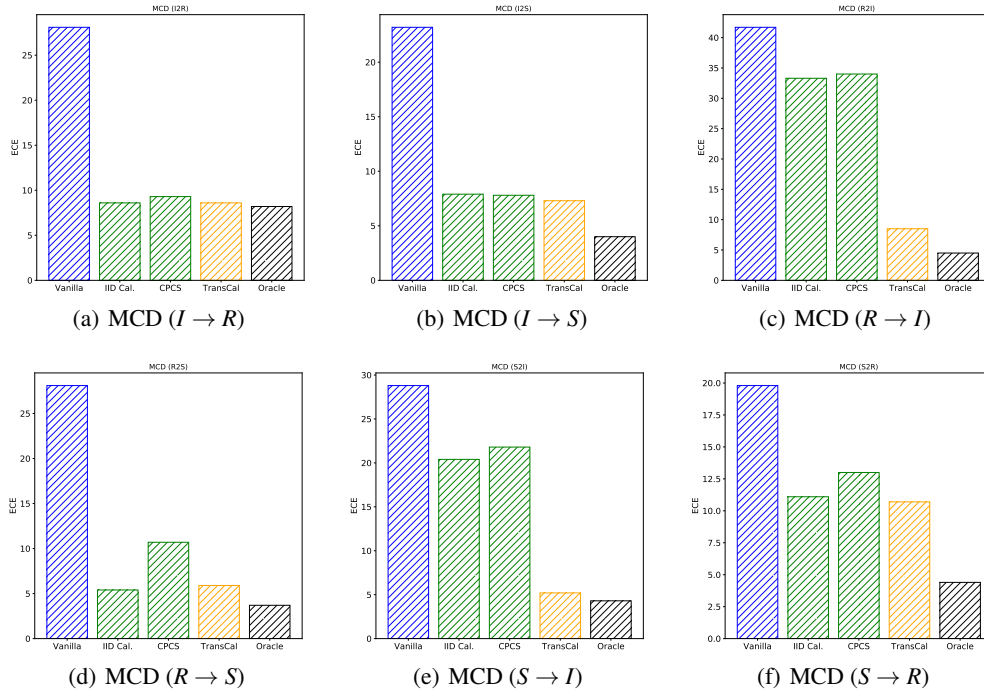


Figure 10: ECE(%) before and after various calibration methods for MCD on *DomainNet*.

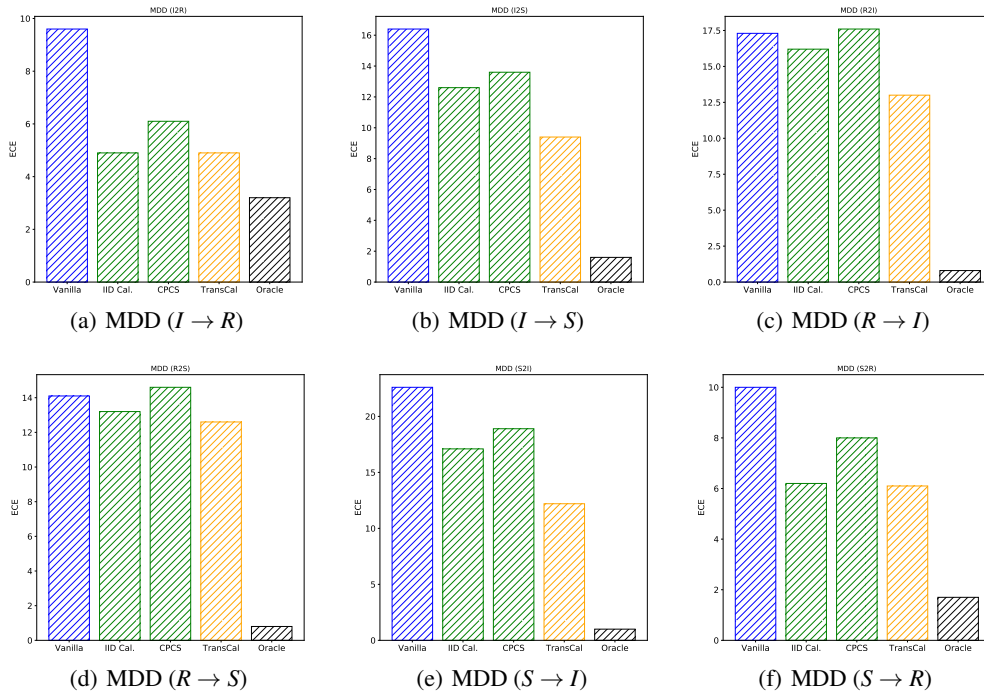


Figure 11: ECE(%) before and after various calibration methods for MDD on *DomainNet*.

D.2.4 Evaluated by Negative Log-Likelihood (NLL)

In Section 4.2 of the main paper, we report ECE after recalibrating various domain adaptation methods on various datasets using TransCal. To verify that TransCal can also perform on other calibration metrics while only optimizing on ECE, we report the results of TransCal on NLL. As shown in Table 7, TransCal also outperforms other calibration methods when evaluated by NLL.

Table 7: NLL before and after various calibration methods for various tasks on *Office-Home*.

Method	Transfer Task	A→C	A→P	A→R	C→A	C→P	C→R	Avg
MDD	Before Cal. (Vanilla)	3.94	2.13	2.13	2.97	2.39	1.87	2.57
	IID Cal. (Temp. Scaling)	3.13	1.80	1.71	2.20	1.75	1.42	2.00
	CPCS [39]	3.23	1.91	1.73	2.27	1.76	<u>1.41</u>	2.05
	TransCal (w/o Bias)	2.62	1.62	1.68	2.31	1.64	1.45	1.89
	TransCal (w/o Variance)	<u>2.51</u>	<u>1.41</u>	<u>1.37</u>	2.18	<u>1.54</u>	1.42	<u>1.74</u>
	TransCal (ours)	2.20	1.31	1.36	<u>2.20</u>	1.48	1.40	1.66
	Oracle	2.13	1.31	1.35	1.79	1.47	1.28	1.56
MCD	Before Cal. (Vanilla)	3.89	2.57	1.62	3.01	2.45	1.70	2.54
	IID Cal. (Temp. Scaling)	2.67	1.96	1.28	2.14	1.86	1.33	1.87
	CPCS [39]	2.71	1.97	1.28	2.09	1.85	1.33	1.87
	TransCal (w/o Bias)	2.60	2.26	1.30	<u>2.06</u>	1.67	1.32	1.87
	TransCal (w/o Variance)	<u>2.56</u>	1.87	1.18	2.12	<u>1.66</u>	1.33	<u>1.79</u>
	TransCal (ours)	2.51	<u>1.89</u>	<u>1.19</u>	1.99	1.65	1.32	1.76
	Oracle	2.46	1.70	1.17	1.93	1.65	1.31	1.70

D.2.5 Evaluated by Brier Score (BS)

Similarly, we further report the results of TransCal on BS. As shown in Table 8, TransCal outperforms its competitors on various datasets and domain adaptation methods when evaluated by BS. Note that, no matter which kind of calibration metrics we adopt to evaluate the performance, TransCal is only optimized via the proposed importance weighted expected calibration error metric.

Table 8: BS before and after various calibration methods for various tasks on *Office-Home*.

Method	Transfer Task	A→C	A→P	A→R	C→A	C→P	C→R	Avg
MDD	Before Cal. (Vanilla)	0.780	0.455	0.455	0.683	0.542	0.491	0.568
	IID Cal. (Temp. Scaling)	0.739	0.442	0.438	<u>0.630</u>	0.501	0.452	0.534
	CPCS [39]	0.745	0.447	0.438	<u>0.637</u>	0.502	<u>0.451</u>	0.537
	TransCal (w/o Bias)	0.699	0.433	0.436	0.640	0.491	0.456	0.526
	TransCal (w/o Variance)	<u>0.687</u>	<u>0.422</u>	0.419	0.628	<u>0.480</u>	0.452	<u>0.515</u>
	TransCal (ours)	0.647	0.420	0.419	<u>0.630</u>	0.473	0.449	0.506
	Oracle	0.635	0.419	0.419	0.577	0.473	0.432	0.493
MCD	Before Cal. (Vanilla)	0.914	0.635	0.452	0.748	0.617	0.512	0.647
	IID Cal. (Temp. Scaling)	0.790	0.595	0.420	0.670	0.575	0.463	0.586
	CPCS [39]	0.796	0.597	0.421	0.661	0.573	0.463	0.585
	TransCal (w/o Bias)	0.776	0.620	0.424	<u>0.655</u>	0.546	0.461	0.580
	TransCal (w/o Variance)	<u>0.768</u>	0.585	0.394	0.666	<u>0.542</u>	0.463	<u>0.570</u>
	TransCal (ours)	0.756	<u>0.588</u>	<u>0.396</u>	0.641	0.540	<u>0.462</u>	0.564
	Oracle	0.743	0.558	0.393	0.622	0.540	0.455	0.552

D.3 More Qualitative Results.

Here, we further report more reliability diagrams for more DA tasks in Figure 12, Figure 13, Figure 14, Figure 15, Figure 16, Figure 17 respectively, showing that TransCal performs much better.

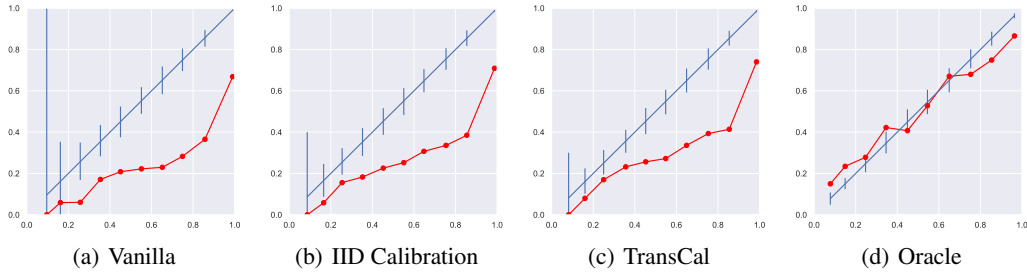


Figure 12: Reliability diagrams for the model from *Art* to *Clipart* before and after calibration.

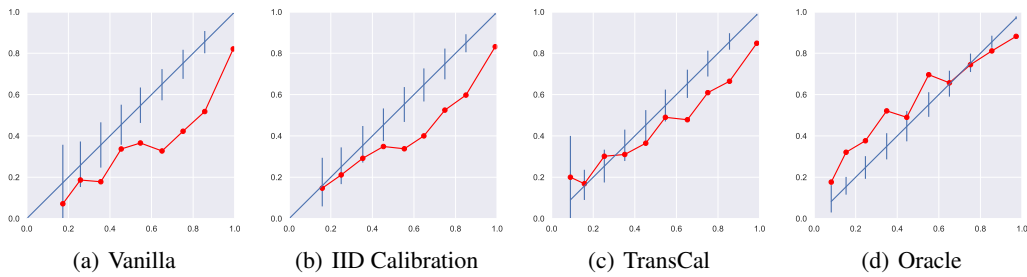


Figure 13: Reliability diagrams for the model from *Art* to *Product* before and after calibration.

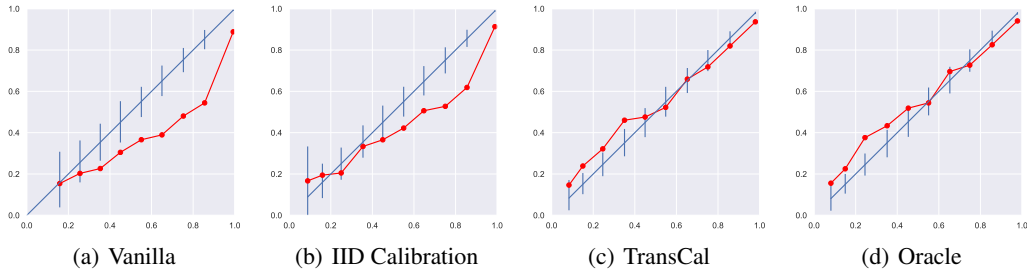


Figure 14: Reliability diagrams for the model from *Art* to *Real-World* before and after calibration.

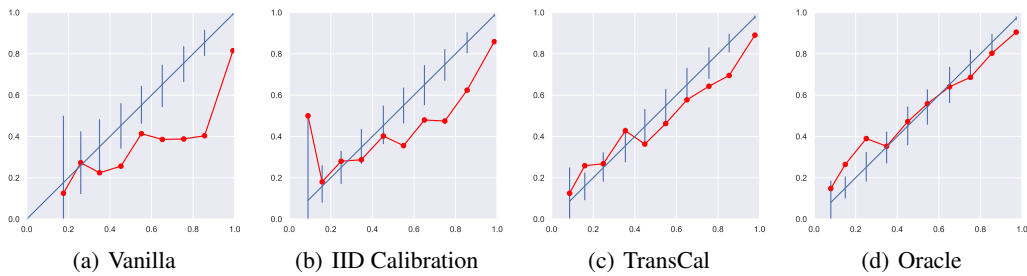


Figure 15: Reliability diagrams for the model from *Real-World* to *Art* before and after calibration.

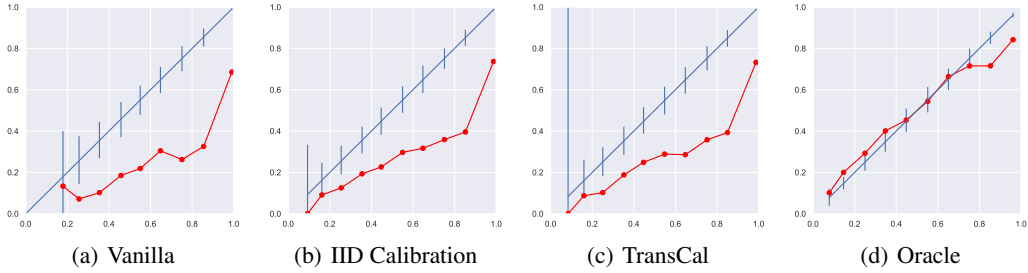


Figure 16: Reliability diagrams for the model from *Real-World* to *Clipart* before and after calibration.

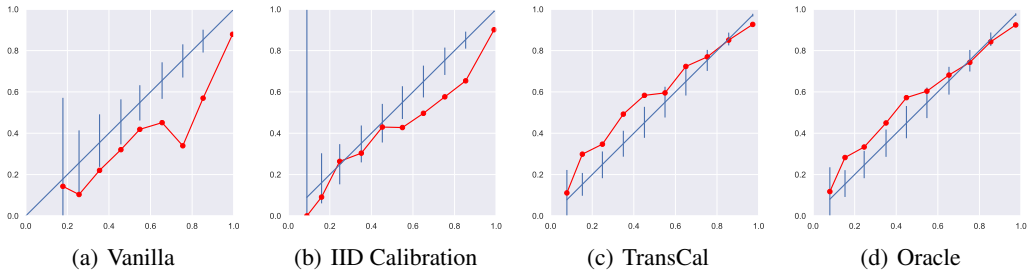


Figure 17: Reliability diagrams for the model from *Real-World* to *Product* before and after calibration.

E Future Work

As mentioned above, TransCal works well across many transfer tasks with various DA models. However, it may still fall short under the following circumstances: 1) The domain gap is extremely large even after applying domain adaptation methods; 2) The source or the target dataset is too small to give an accurate importance weighting estimation; 3) Since TransCal is based on the covariate shift assumption, it remains unclear whether it can still perform well under label shift, especially when we meet with a long-tailed distribution. We leave them as future work.